

State-dependency of
the equilibrium
climate sensitivity

P. Köhler et al.

On the state-dependency of the equilibrium climate sensitivity during the last 5 million years

P. Köhler¹, B. de Boer^{2,3}, A. S. von der Heydt³, L. B. Stap³, and R. S. W. van de Wal³

¹Alfred-Wegener-Institut Helmholtz-Zentrum für Polar-und Meeresforschung (AWI), P.O. Box 12 01 61, 27515 Bremerhaven, Germany

²Department of Earth Sciences, Faculty of Geosciences, Utrecht University, Budapestlaan 4, 3584 CD Utrecht, the Netherlands

³Institute for Marine and Atmospheric Research Utrecht (IMAU), Utrecht University, Princetonplein 5, 3584 CC Utrecht, the Netherlands

Received: 02 June 2015 – Accepted: 22 June 2015 – Published: 10 July 2015

Correspondence to: P. Köhler (peter.koehler@awi.de)

Published by Copernicus Publications on behalf of the European Geosciences Union.

Title Page

Abstract

Introduction

Conclusions

References

Tables

Figures



Back

Close

Full Screen / Esc

Printer-friendly Version

Interactive Discussion



Abstract

A still open question is how equilibrium warming in response to increasing radiative forcing – the specific equilibrium climate sensitivity S – is depending on background climate. We here present paleo-data based evidence on the state-dependency of S , by using CO_2 proxy data together with 3-D ice-sheet model-based reconstruction of land ice albedo over the last 5 million years (Myr). We find that the land-ice albedo forcing depends non-linearly on the background climate, while any non-linearity of CO_2 radiative forcing depends on the CO_2 data set used. This non-linearity was in similar approaches not accounted for due to previously more simplistic approximations of land-ice albedo radiative forcing being a linear function of sea level change. Important for the non-linearity between land-ice albedo and sea level is a latitudinal dependency in ice sheet area changes. In our setup, in which the radiative forcing of CO_2 and of the land-ice albedo (LI) is combined, we find a state-dependency in the calculated specific equilibrium climate sensitivity $S_{[\text{CO}_2, \text{LI}]}$ for most of the Pleistocene (last 2.1 Myr). During Pleistocene intermediate glaciated climates and interglacial periods $S_{[\text{CO}_2, \text{LI}]}$ is on average $\sim 45\%$ larger than during Pleistocene full glacial conditions. In the Pliocene part of our analysis (2.6–5 MyrBP) the CO_2 data uncertainties prevents a well-supported calculation for $S_{[\text{CO}_2, \text{LI}]}$, but our analysis suggests that during times without a large land-ice area in the Northern Hemisphere (e.g. before 2.82 MyrBP) the specific equilibrium climate sensitivity $S_{[\text{CO}_2, \text{LI}]}$ was smaller than during interglacials of the Pleistocene. We thus find support for a previously proposed state-change in the climate system with the wide appearance of northern hemispheric ice sheets. This study points for the first time to a so far overlooked non-linearity in the land-ice albedo radiative forcing, which is important for similar paleo data-based approaches to calculate climate sensitivity. However, the implications of this study for a suggested warming under CO_2 doubling are not yet entirely clear since the necessary corrections for other slow feedbacks are in detail unknown and the still existing uncertainties in the ice sheet simulations and global temperature reconstructions are large.

State-dependency of the equilibrium climate sensitivity

P. Köhler et al.

Title Page

Abstract

Introduction

Conclusions

References

Tables

Figures



Back

Close

Full Screen / Esc

Printer-friendly Version

Interactive Discussion



1 Introduction

One measure to describe the potential anthropogenic impact on climate is the equilibrium global annual mean surface air temperature rise caused by the radiative forcing of a doubling of atmospheric CO₂ concentration. While this quantity, called equilibrium climate sensitivity (ECS), can be calculated from climate models (e.g. Vial et al., 2013), it is for model validation important to make estimates based on paleo-data. This is especially relevant since some important feedbacks of the climate system are not incorporated in all models. For example, when coupling a climate model interactively to a model of stratospheric chemistry, including ozone, the calculated transient warming on a hundred-years time scale differs by 20 % from results without such an interactive coupling (Nowack et al., 2015).

Both approaches, model-based (Stocker et al., 2013) and data-based (PALAEOSENS-Project Members, 2012; Hansen et al., 2013), still span a wide range for ECS e.g. of 1.9–4.4 K (90 % confidence interval) in the most recent simulations compiled in the IPCC assessment report (Stocker et al., 2013), or 2.2–4.8 K (68 % probability) in a paleo data compilation covering examples from the last 65 million years (PALAEOSENS-Project Members, 2012). Reducing the uncertainty in ECS is challenging, but some understanding on model-based differences now emerges (Vial et al., 2013; Shindell, 2014).

The ultimate cause for orbital-scale climate change are latitudinal and seasonal changes in the incoming solar radiations (Milankovitch, 1941; Laskar et al., 2004), which are then amplified by various feedbacks in the climate system (Hays et al., 1976). These details in incoming solar radiation are not resolved in our approach, which focuses on the contribution of various climate feedbacks to the reconstructed changes (PALAEOSENS-Project Members, 2012). When using paleo-data to calculate climate sensitivity one has to correct for slow feedbacks, whose impacts on climate are incorporated in the temperature reconstructions. Slow feedbacks are of interest in a more distant future (Zeebe, 2013), but are not yet considered in climate simula-

CPD

11, 2019–2069, 2015

State-dependency of the equilibrium climate sensitivity

P. Köhler et al.

Title Page

Abstract

Introduction

Conclusions

References

Tables

Figures



Back

Close

Full Screen / Esc

Printer-friendly Version

Interactive Discussion



State-dependency of the equilibrium climate sensitivity

P. Köhler et al.

Title Page

Abstract

Introduction

Conclusions

References

Tables

Figures



Back

Close

Full Screen / Esc

Printer-friendly Version

Interactive Discussion



tions using fully coupled climate models underlying the fifth assessment report of the IPCC (Stocker et al., 2013). More generally, from paleo-data the specific equilibrium climate sensitivity $S_{[X]}$ is calculated, which is, in line with the proposed nomenclature of PALAEOSSENS-Project Members (2012), the ratio of the equilibrium global (g) surface temperature change ΔT_g over the specific radiative forcing ΔR of the processes X , hence $S_{[X]} = \Delta T_g \cdot \Delta R_{[X]}^{-1}$. In this concept “slow feedbacks” are considered as forcing. The division in “forcing” and “feedback” is based on the time scale of the process. PALAEOSSENS-Project Members (2012) found that a century is a well justified time scale that might distinguish fast feedbacks from slow forcings. All relevant processes that are not considered in the forcing term X will impact on climate change as feedbacks. This has to be kept in mind for comparing model-based and data-based approaches and makes their comparison difficult, since in model-based results only those processes implemented in the model have an impact on calculated temperature change.

In practical terms, the paleo-data that are typically available for the calculation of S are the radiative forcing of CO_2 and surface albedo changes caused by land ice (LI) sheets. Thus $S_{[\text{CO}_2, \text{LI}]}$ can be calculated containing the radiative forcing of two processes, which are most important during glacial/interglacial timescales of the late Pleistocene (Köhler et al., 2010). The whole approach therefore relies on the simplification that the climate response of the CO_2 radiative forcing and the surface albedo radiative forcing are similar. We are aware that such a simplification might not be possible for every radiative forcing, since Shindell (2014) showed that the per unit radiative forcing of well-mixed greenhouse gases (e.g. CO_2 or CH_4) leads to a different climate response than that of aerosols or ozone. However, we are not aware that a difference in the response has been shown for radiative forcing from surface albedo changes ($\Delta R_{[\text{LI}]}$) and CO_2 ($\Delta R_{[\text{CO}_2]}$). Hence we combine them linearly.

Both model-based (e.g. Crucifix, 2006; Hargreaves et al., 2007; Yoshimori et al., 2011; Caballero and Huber, 2013; Goldner et al., 2013; Kutzbach et al., 2013; Meraner et al., 2013) and paleo-data-based (PALAEOSSENS-Project Members, 2012) ap-

State-dependency of the equilibrium climate sensitivity

P. Köhler et al.

Title Page

Abstract

Introduction

Conclusions

References

Tables

Figures



Back

Close

Full Screen / Esc

Printer-friendly Version

Interactive Discussion



system with respect to previous studies. Third, previously (e.g. van de Wal et al., 2011) polar amplification was assumed to be constant over time. However, climate models (Haywood et al., 2013) indicate that during the Pliocene, when less ice was present on the Northern Hemisphere, the temperature perturbations were more uniformly spread
 5 over all latitudes. We incorporate this changing polar amplification in our global temperature record. Fourth, we explicitly analyse for the first time whether the relationship between temperature change and radiative forcing is better described by a linear or non-linear function. If the applied statistics inform us that the ΔT_g – ΔR -relationship contains a non-linearity, then the specific equilibrium climate sensitivity is state-dependent.
 10 Any knowledge on a state-dependency of S is important for the interpretation of paleo data and for the projection of long-term future climate change.

2 Methods

We calculate the radiative forcing of CO_2 and land-ice albedo, $\Delta R_{[\text{CO}_2, \text{LI}]}$, by applying the same energy balance model as used before for the late Pleistocene (Köhler et al., 2010). This approach uses CO_2 data from ice cores and based on different proxies
 15 from three different labs published for the last 5 Myr and calculates changes in surface albedo from zonal averaged changes in land ice area. The latter are here based on results from 3-D ice-sheet model simulations (de Boer et al., 2014), that deconvolved the benthic $\delta^{18}\text{O}$ stack LR04 (Lisiecki and Raymo, 2005) into its temperature and sea level (ice volume) component. The time series of global temperature change ΔT_g over
 20 the last 5 Myr used here is also based on this deconvolution. The reconstructed records of ice volume and temperature changes are therefore mutually consistent.

2.1 Ice-sheet models, changes in surface albedo and radiative forcing $\Delta R_{[\text{LI}]}$

Using an inverse modelling approach and the 3-D ice-sheet model ANICE (de Boer et al., 2014) the benthic $\delta^{18}\text{O}$ stack LR04 (Lisiecki and Raymo, 2005) is deconvolved
 25

in deep-ocean temperature, eustatic sea-level variations, and a representation of the four main ice sheets in Antarctica, Greenland, Eurasia, and North America. The spatial resolution (grid cell size) for the Antarctic, Eurasian and North American ice sheets is 40 km × 40 km, while Greenland is simulated by cells of 20 km × 20 km.

This approach combines paleo-data and mass conservation for $\delta^{18}\text{O}$ with physical knowledge on ice sheet growth and decay. It therefore includes a realistic estimate of both volume and surface area of the major ice sheets. The calculated change in deep-ocean temperature is in this ice sheet-centred approach connected with temperature anomalies over land in the Northern Hemisphere (NH) high latitude band (40–85°N, ΔT_{NH}), in which the Greenland, Eurasian, and North American ice sheets grow. Temporal resolution of all simulation results from the 3-D ice-sheet models is 2 kyr.

From these results, published previously (de Boer et al., 2014) the latitudinal distribution of land-ice area is calculated (Fig. 1b), which leads to changes in surface albedo and the land-ice sheet-based radiative forcing, $\Delta R_{[\text{LI}]}$, with respect to preindustrial times. $\Delta R_{[\text{LI}]}$ is now calculated from local annual mean insolation at the top of the atmosphere (TOA), I_{TOA} , and changes in ice-sheet area in latitudinal bands of 5° (Fig. 1) and globally integrated thereafter. This approach to calculate $\Delta R_{[\text{LI}]}$ is based on surface albedo anomalies, implying that always ice-free latitudes contribute nothing to $\Delta R_{[\text{LI}]}$. It is assumed that ice sheets cover land when growing, thus local surface albedo rises as applied previously (Köhler et al., 2010) from 0.2 to 0.75. For calculating I_{TOA} (Fig. 1a), which varies due to orbital configurations (Laskar et al., 2004), we use a solar constant of 1360.8 W m^{-2} , the mean of more than 10 years of daily data satellite since early 2003 as published by the SORCE project (<http://lasp.colorado.edu/home/sorce>) (Kopp and Lean, 2011). Changes in solar energy output are not considered, but are based on present knowledge (Roth and Joos, 2013) smaller than 1 W m^{-2} during the last 10 kyr, and, following our earlier approach (Köhler et al., 2010), presumably smaller than 0.2%.

For validation of the ANICE ice sheet model we compare the spatial and temporal variable results in $\Delta R_{[\text{LI}]}$ obtained for Termination I (the last 20 kyr) with those based

State-dependency of the equilibrium climate sensitivity

P. Köhler et al.

Title Page

Abstract

Introduction

Conclusions

References

Tables

Figures



Back

Close

Full Screen / Esc

Printer-friendly Version

Interactive Discussion



on the land ice sheet distribution of ICE-5G (Peltier, 2004). For this comparison the ICE-5G data are treated similarly as those from ANICE, e.g. only data every 2kyr are considered and averaged on latitudinal bands of 5° . The spatial distribution of land ice in the most recent version of ICE-6G (Peltier et al., 2015) are similar to ICE-5G and therefore no significant difference to ICE-6G are expected and the comparison to that version is omitted.

2.2 Global temperature change ΔT_g

We calculate global surface temperature change ΔT_g from NH temperature anomalies, ΔT_{NH} , using a polar amplification (pa) factor f_{pa} which itself depends on climate (Fig. 2). Based on results from two modelling inter-comparison projects f_{pa} was determined to be 2.7 ± 0.3 for the Last Glacial Maximum (LGM, about 20 kyr BP) (PMIP3/CMIP5 (Braconnot et al., 2012)) and 1.6 ± 0.1 for the mid Pliocene Warm Period (mPWP, about 3.2 Myr BP) (PlioMIP (Haywood et al., 2013)). In our standard setup (calculating ΔT_{g1}) we linearly inter- and extrapolate f_{pa} as function of ΔT_{NH} based on these two anchor values for all background climates found during the last 5 Myr (insert in Fig. 2a). Climate models already suggest that polar amplification is not constant, but how it is changing over time is not entirely clear (Masson-Delmotte et al., 2006; Abe-Ouchi et al., 2007; Hargreaves et al., 2007; Yoshimori et al., 2009; Singarayer and Valdes, 2010). We therefore calculate an alternative global temperature change ΔT_{g2} in which we assume polar amplification f_{pa} to be a step function, with $f_{pa} = 1.6$ (the mPWP value) taken for times with large northern hemispheric land ice (according to our results before 2.82 Myr BP), and with $f_{pa} = 2.7$ (the LGM value) thereafter. This choice is motivated by investigations with a coupled ice sheet-climate model, from which northern hemispheric land ice was identified to be the main controlling factor for the polar amplification (Stap et al., 2014).

At the LGM ΔT_g was, based on the eight PMIP3 models contributing to this estimate in f_{pa} , -4.6 ± 0.8 K, so slightly colder, but well overlapping the most recent LGM estimate (Annan and Hargreaves, 2013) of $\Delta T_g = -4.0 \pm 0.8$ K. If we take into con-

State-dependency of the equilibrium climate sensitivity

P. Köhler et al.

Title Page

Abstract

Introduction

Conclusions

References

Tables

Figures



Back

Close

Full Screen / Esc

Printer-friendly Version

Interactive Discussion



5 tigate the robustness of our approach to the selected time series. As can be seen in the results our main conclusions and functional dependencies are independent from the choice of ΔT_g and are also supported if based on either ΔT_{g2} or ΔT_{g3} (see Table 1).

10 The modelled surface–air temperature change ΔT_{NH} was already compared (de Boer et al., 2014) with three independent proxy-based records of sea surface temperature (SST) change in the North Atlantic (Lawrence et al., 2009), equatorial Pacific (Herbert et al., 2010) and Southern Ocean (Martínez-García et al., 2010) which cover at least the last 3.5 Myr. The main features of the simulated temperature change and the data-based SST reconstruction agree: the overall cooling trend from about 3.5 to 1 Myr ago is found in the simulation results and in all SST records, so is the strong glacial–interglacial (100 kyr) variability thereafter.

2.3 Radiative forcing of CO₂, $\Delta R_{[CO_2]}$

15 Several labs developed different proxy-based approaches to reconstruct atmospheric CO₂ before the ice-core time window of the last 0.8 Myr. Since we are interested how CO₂ might have changed over the last 5 Myr and on its relationship to global climate we only consider longer time series for our analysis. Thus, some approaches, e.g. based on stomata, with only a few data points during the last 5 Myr are not considered (see Beerling and Royer, 2011). The considered CO₂ data are in detail (Fig. 3):

- 20 a. ice core CO₂ data were compiled by Bereiter et al. (2015) into a stacked ice core CO₂ record covering the last 0.8 Myr including a revision of the CO₂ data from the lowest part of the EPICA Dome C ice core. Originally, the stack as published (Bereiter et al., 2015) contains 1723 data points before year 1750 CE, the beginning of the industrialisation, but was here resampled to the 2 kyr time step of the ice-sheet simulation results by averaging available data points, and reducing the sample size to $n = 394$. The stack contains data from the ice cores at Law Dome (Rubino et al., 2013; MacFarling-Meure et al., 2006) (0–2 kyr BP), EPICA Dome C (Monnin et al., 2001, 2004; Schneider et al., 2013; Siegenthaler
- 25

State-dependency of the equilibrium climate sensitivity

P. Köhler et al.

Title Page

Abstract

Introduction

Conclusions

References

Tables

Figures



Back

Close

Full Screen / Esc

Printer-friendly Version

Interactive Discussion



State-dependency of the equilibrium climate sensitivity

P. Köhler et al.

Title Page

Abstract Introduction

Conclusions References

Tables Figures

◀ ▶

◀ ▶

Back Close

Full Screen / Esc

Printer-friendly Version

Interactive Discussion



Discussion Paper | Discussion Paper | Discussion Paper | Discussion Paper | Discussion Paper

et al., 2005; Bereiter et al., 2015) (2–11 kyrBP, 104–155 kyrBP, 393–806 kyrBP), West Antarctic Ice Sheet Divide (Marcott et al., 2014) (11–22 kyrBP), Siple Dome (Ahn and Brook, 2014) (22–40 kyrBP), Talos Dome (Bereiter et al., 2012) (40–60 kyrBP), EPICA Donning Maud Land (Bereiter et al., 2012) (60–104 kyrBP) and Vostok (Petit et al., 1999) (155–393 kyrBP).

- b. CO₂ based on δ¹¹B isotopes measured on planktonic shells of *G. sacculifer* from the Hönisch-lab (Hönisch et al., 2009) (*n* = 52) is obtained from ODP668B located in the eastern equatorial Atlantic. The data go back until 2.1 MyrBP and agree favourably with the ice core CO₂ during the last 0.8 Myr.
- c. CO₂ data from the Foster-lab (Foster, 2008; Martínez-Botí et al., 2015) are available for the last 3.3 Myr (*n* = 105) obtained via δ¹¹B from ODP site 999 in the Caribbean Sea. CO₂ purely based on *G. ruber* δ¹¹B was reconstructed for the last glacial cycle (Foster, 2008) and for about 0.8 Myr during the Plio–Pleistocene transition (Martínez-Botí et al., 2015). We take both these data sets using identical calibration as plotted previously (Martínez-Botí et al., 2015). The overlap of the data with the ice core CO₂ is reasonable with the tendency for overestimating the maximum anomalies in CO₂ (by more than +50 ppmv during warm previous interglacials and by –25 ppmv during the LGM, Fig. 3b).
- d. CO₂ reconstructions based on alkenone from the Pagani-lab (Pagani et al., 2010; Zhang et al., 2013) (*n* = 153) cover the whole 5 Myr and are derived from different marine sediment cores. Site 925 is contained in both publications, although with different uncertainties. From site 925 we use the extended and most recent CO₂ data of Zhang et al. (2013) containing 50 data points over the last 5 Myr, 18 points more than initially published. Data from the sites 806, 925 and 1012 are offset from the ice core CO₂ reference during the last 0.8 Myr by +50 to +100 ppmv, while data from site 882 have no overlapping data points with the ice cores. It is not straightforward how these CO₂ data from the Pagani-lab that are offset from

the ice core CO₂ might be corrected. Therefore, we refrain from applying any corrections but keep these offsets in mind for our interpretation.

Other CO₂ data based on B/Ca (Tripathi et al., 2009) are not considered here, since critical issues concerning its calibration have been raised (Allen et al., 2012). A second $\delta^{11}\text{B}$ -based record of the Hönisch-lab (Bartoli et al., 2011) from *G. sacculifer* obtained from ODP site 999 is not used for further analysis, because $\delta^{11}\text{B}$ was measured on other samples than proxies that are necessary to determine the related climate state (e.g. $\delta^{18}\text{O}$). Thus, a clear identification if glacial or interglacial conditions were prevailing for individual data points was difficult. Furthermore, these calculated CO₂ values (Bartoli et al., 2011) have very high uncertainties, 1σ is $3\times$ larger than in the original Hönisch-lab data set (Hönisch et al., 2009). These CO₂ data of Bartoli et al. (2011) disagrees with the most recent data from the Foster-lab (Martínez-Botí et al., 2015), especially before the onset of northern hemispheric glaciation around 2.8Myr ago. Another CO₂ time series from the Foster-lab (Seki et al., 2010) based on a mixture of both alkenones or $\delta^{11}\text{B}$ approaches covering the last 5 Myr is not considered here, since the applied size-correction for the alkenone producers has subsequently been shown to be incorrect (Badger et al., 2013).

Radiative forcing based on CO₂ is calculated using $\Delta R_{[\text{CO}_2]} = 5.35 \text{ W m}^{-2} \cdot \ln(\text{CO}_2/\text{CO}_{2,0})$ with CO_{2,0} = 278 ppmv being the preindustrial reference value (Myhre et al., 1998).

2.4 How to calculate the specific equilibrium climate sensitivity $S_{[\text{CO}_2, \text{LI}]}$

The specific equilibrium climate sensitivity for a forcing X is defined as $S_{[X]} = \Delta T_g \cdot \Delta R_{[X]}^{-1}$. In an analysis of $S_{[X]}$ when calculated for every point in time for the last 0.8 Myr based on ice core data PALAEOSENS-Project Members (2012) revealed the range of possible values, which fluctuated widely not following a simple functionality, even when analysed as moving averages. This study also clarified that $S_{[X]}$ based on small disturbances in ΔT_g or $\Delta R_{[X]}$ are due to dating uncertainties prone to unrealistic high/low

State-dependency of the equilibrium climate sensitivity

P. Köhler et al.

Title Page

Abstract

Introduction

Conclusions

References

Tables

Figures



Back

Close

Full Screen / Esc

Printer-friendly Version

Interactive Discussion



values. Only when data are analysed in a scatter-plot a non-linear functionality between ΔT_g and $\Delta R_{[X]}$, and therefore a state-dependency of $S_{[X]}$, emerges as signal out of the noisy data (von der Heydt et al., 2014).

Here, ΔT_g is approximated as a function of $\Delta R_{[X]}$ by fitting a non-linear function (a polynomial up to the third order, $y(x) = a + bx + cx^2 + dx^3$) to the scattered data of ΔT_g vs. $\Delta R_{[X]}$. The individual contribution of land ice albedo and CO₂ to a state-dependency of $S_{[CO_2,LI]}$ can be investigated by analysing both $S_{[CO_2]}$ and $S_{[CO_2,LI]}$. If the best fit follows a linear function, e.g. for state-independent behaviour of $S_{[X]}$, its values might be determined from the slope of the regression line in the ΔT_g - $\Delta R_{[X]}$ -space. However, note that here a necessary condition for the calculation of $S_{[X]}$ over the whole range of $\Delta R_{[X]}$, but not for the analysis of any state-dependency is, that any fitting function crosses the origin with $\Delta R_{[CO_2,LI]} = 0 \text{ W m}^{-2}$ and $\Delta T_g = 0 \text{ K}$, implying for the fitting parameters that $a = 0$. This is also in line with the general concept that without any change in the external forcing no change in global mean temperature should appear. Since the data sets have apparent offsets from the origin we first investigate which order of the polynomial best fits the data by allowing parameter a to vary from 0.

For the calculation of mean values of $S_{[CO_2,LI]}$ we then analyse in a second step the $S_{[CO_2,LI]}-\Delta R_{[CO_2,LI]}$ -space, where $S_{[CO_2,LI]} = \Delta T_g \cdot \Delta R_{[CO_2,LI]}^{-1}$ is first calculated individually for every data point and then stacked for different background conditions (described by $\Delta R_{[CO_2,LI]}$). In doing so we circumvent the problem that the regression function needs to meet the origin, that appeared in the $\Delta T_g-\Delta R_{[X]}$ -space. Some of the individual values of $S_{[CO_2,LI]}$ are still unrealistically high/low, therefore values in $S_{[CO_2,LI]}$ outside the plausible range of $0-3 \text{ KW}^{-1} \text{ m}^2$ are rejected from further analysis.

The scattered data of $S_{[CO_2,LI]}$ as function of $\Delta R_{[CO_2,LI]}$ are then compiled in a probability density function (PDF), in which we also consider the given uncertainties of the individual data points. For the calculation of the PDFs we distinguish between a few different climate states, when supported by the data. For the time being the data cov-

State-dependency of the equilibrium climate sensitivity

P. Köhler et al.

[Title Page](#)[Abstract](#)[Introduction](#)[Conclusions](#)[References](#)[Tables](#)[Figures](#)[Back](#)[Close](#)[Full Screen / Esc](#)[Printer-friendly Version](#)[Interactive Discussion](#)

erage is too sparse and uncertainties are too large to calculate any state-dependent values of $S_{[\text{CO}_2, \text{LI}]}$ in greater detail.

The fitting routines (Press et al., 1992) use the method of general linear least squares. Here, a function $\chi^2 = \sum_i^n \frac{(y_i - y(x))^2}{\sigma_y^2}$ is minimised, which calculates the sum of

squares of the offsets of the fit from the n data points normalised by the average variance σ_y^2 . Since established numerical methods for calculating a non-linear fit through data cannot consider uncertainties in x we base our regression analysis on a Monte-Carlo approach. Data points are randomly picked from the Gaussian distribution described by the given 1σ standard deviation of each data point in both directions x ($\Delta R_{[X]}$) and y (ΔT_g). We generated 5000 of these data sets, calculated their individual non-linear fits and further analysed results based on averages of the regression parameters. The Monte-Carlo approach converges if the number of replicates exceeds 1000, e.g. variations in the mean of the parameters are at least an order of magnitude smaller than the uncertainties connected with the averaging of the results. We used the χ^2 of the fitting routines in F tests to investigate if a higher order polynomial would describe the scattered data in the $(\Delta T_g - \Delta R_{[X]})$ -parameter space better than a lower order polynomial and use the higher order polynomial only if it significantly better describes the data at the 1% level (p value of F test: $p \leq 0.01$, Table 1).

2.5 Uncertainty estimates

As previously described in detail (Köhler et al., 2010) standard error propagation is used to calculate uncertainties in ΔT and ΔR . For $\Delta R_{[\text{LI}]}$ changes in surface albedo are assumed to have a 1σ -uncertainty of 0.1, simulated changes in land-ice-area have in the various simulation scenarios performed in de Boer et al. (2014) a relative uncertainty of 10%. The different approaches to reconstruct CO_2 all have different uncertainties as plotted in Fig. 3. Ice core CO_2 has a 1σ uncertainty of 2 ppmv, while those based on other proxies have individual errors connected with the data-points that are on the order of 20–50 ppmv. Radiative forcing based on CO_2 , $\Delta R_{[\text{CO}_2]} =$

State-dependency of the equilibrium climate sensitivity

P. Köhler et al.

Title Page

Abstract

Introduction

Conclusions

References

Tables

Figures



Back

Close

Full Screen / Esc

Printer-friendly Version

Interactive Discussion



State-dependency of the equilibrium climate sensitivity

P. Köhler et al.

Title Page

Abstract

Introduction

Conclusions

References

Tables

Figures



Back

Close

Full Screen / Esc

Printer-friendly Version

Interactive Discussion



$5.35 \text{ W m}^{-2} \cdot \ln(\text{CO}_2/\text{CO}_{2,0})$ has in addition to the uncertainty in CO_2 itself also another 10% 1σ -uncertainty (Forster et al., 2007). The uncertainty in the incoming insolation is restricted to known variations in the solar constant to be of the order of 0.2%. Annual mean global surface temperature ΔT_g is solely based on the polar amplification factor f_{pa} and ΔT_{NH} . Uncertainty in ΔT_{NH} is estimated based on eight different model realisations of the deconvolution of benthic $\delta^{18}\text{O}$ into sea level and temperature (de Boer et al., 2014). Based on the analysis of the PMIP3 and PlioMIP results the polar amplification factor $f_{\text{pa}} = \Delta T_{\text{NH}} \cdot \Delta T_g^{-1}$ has a relative uncertainty of 10% (see Fig. 2a).

These uncertainties used in an error propagation lead to the $\sigma_{\Delta T_g}$, $\sigma_{\Delta R_{[\text{CO}_2]}}$ and $\sigma_{\Delta R_{[\text{CO}_2, \text{LI}]}}$ of the individual data points and are used to constrain the Monte-Carlo statistics. The stated uncertainties of the parameters of the polynomials fitting the scattered $\Delta T - \Delta R$ -data given in Table 1 and used to plot and calculate $S_{[\text{CO}_2, \text{LI}]}$ are derived from averaging results of the Monte-Carlo approach. Note, that higher order polynomials give more constrains on the parameters and therefore lead to smaller uncertainties.

3 Results

3.1 Individual radiative forcing contributions from land ice albedo and CO_2

We calculate a resulting radiative forcing of CO_2 , $\Delta R_{[\text{CO}_2]}$, that span a range from -2.8 to $+2.5 \text{ W m}^{-2}$ compared to preindustrial conditions (Fig. 4b). The uncertainty in $\Delta R_{[\text{CO}_2]}$ depends on the proxy. It is about 10% in ice cores, and generally less than 0.5 W m^{-2} for other proxies with the exception of some individual points from the Pagan-lab with uncertainties around 1 W m^{-2} .

In contrast to these rather uncertain and patchy results the ice-sheet simulations lead to a continuous time series of surface albedo changes and $\Delta R_{[\text{LI}]}$ ranging between -4 W m^{-2} during ice ages of the late Pleistocene and $+1 \text{ W m}^{-2}$ during interglacials of the Pliocene (Fig. 4c). During warmer than preindustrial climate $\Delta R_{[\text{LI}]}$ is thus rather

small and between 4.2 and 3.0 Myr ago only slightly higher than $\Delta R_{[\text{orbit}]}$, the radiative forcing due to global annual mean insolation changes caused by variations in the orbital parameters of the solar system (Laskar et al., 2004) (Fig. 4c).

Reconstructed $\Delta R_{[\text{LI}]}$ for the last 20 kyr agrees reasonable well with an alternative based on the ICE-5G ice sheet reconstruction of Peltier (2004) (Fig. 5). Changes in land ice fraction in the northern high latitudes around 15 kyr are more abrupt around 70° N in ICE-5G than in ANICE (Fig. 5b, e). The northward retreat of the southern edge of the NH ice sheets happens later in ICE-5G than in ANICE. In combination, both effects lead to only small differences in the spatial and temporal distribution of the radiative forcing $\Delta R_{[\text{LI}]}$ when based on either ANICE or ICE-5G (Fig. 5c and f).

The ice-albedo forcing $\Delta R_{[\text{LI}]}$ has a non-linear relationship to sea level change (Fig. 6a), which is caused by the use of the sophisticated 3-D ice-sheet models. Hence other approaches which approximate $\Delta R_{[\text{LI}]}$ directly from sea level (Hansen et al., 2008; Martínez-Botí et al., 2015), simpler 1-D ice sheet models or calculate $\Delta R_{[\text{LI}]}$ from global land ice area changes without considering latitudinal dependency (Köhler et al., 2010; von der Heydt et al., 2014) lack an important non-linearity of the climate system. This non-linearity in the $\Delta R_{[\text{LI}]}$ -sea level relationship is also weakly contained in results based on ICE-5G for Termination I (Fig. 6a). However, when plotting identical time steps of Termination I from results based on ANICE, the non-linearity is not yet persisting. This implies, that a larger pool of results from various different climates need to be averaged in order to obtain a statistically robust functional relationship between $\Delta R_{[\text{LI}]}$ and sea level (as done in this study).

The combined forcing $\Delta R_{[\text{CO}_2, \text{LI}]}$ can only be obtained for the data points for which CO₂ data exist (Fig. 4d). The combined forcing ranges from -6 to -7 W m^{-2} during the Last Glacial Maximum (LGM) to, in general, positive values during the Pliocene with a maximum of $+3 \text{ W m}^{-2}$. Between 5.0 and 2.7 Myr ago (most of the Pliocene) the ice sheet area and $\Delta R_{[\text{LI}]}$ are continuously smaller than today, apart from two exceptions around 3.3 Myr and after 2.8 Myr ago, (Fig. 4c) suggesting warmer temperatures

State-dependency of the equilibrium climate sensitivity

P. Köhler et al.

Title Page

Abstract

Introduction

Conclusions

References

Tables

Figures



Back

Close

Full Screen / Esc

Printer-friendly Version

Interactive Discussion



throughout. Proxy data suggest that CO_2 and $\Delta R_{[\text{CO}_2]}$ were in the Pliocene mostly higher than during preindustrial times.

3.2 Detecting any state-dependency in $S_{[\text{CO}_2, \text{LI}]}$

As explained in detail in Sect. 2.4 $S_{[\text{CO}_2, \text{LI}]}$ can be considered state-dependent if the scattered data of ΔT_g against $\Delta R_{[\text{CO}_2, \text{LI}]}$ are better described by a non-linear rather than a linear fit. The plots for the different CO_2 approaches reveal proxy-specific results (Fig. 7). Ice core data ($r^2 = 0.72$) are best described by a third order polynomial, the Hönisch data ($r^2 = 0.79$) by a second order polynomial, while for the Foster ($r^2 = 0.61$) and Pagani ($r^2 = 0.45$) data a second order fit is not statistically significantly better than a linear fit (Table 1).

The fit through the Hönisch data agrees more with the fit through the ice core CO_2 data than with the fit through the other CO_2 -proxy-based approaches, however the Hönisch data set extends only 2.1 Myr back in time and contains no CO_2 data in the warm Pliocene. Thus, the finding of a state-dependency in climate sensitivity obtained from the ice core data covering predominately colder than present periods which we find here – and for which a first indication was published in von der Heydt et al. (2014) – is extended to the last 2.1 Myr, where the climate states similar to the present climate are better sampled than in the the late Pleistocene record as used in von der Heydt et al. (2014). However, we can still not extrapolate this finding to the warmer than present climates of the last 5 Myr since the ice core and Hönisch data do not cover these periods and the Foster and Pagani data do not suggest a similar relationship. These findings remain qualitatively the same if our analyses are based on the alternative global temperature changes ΔT_{g2} or ΔT_{g3} (Table 1).

When analysing the contribution from land ice albedo ($\Delta R_{[\text{LI}]}$) and CO_2 radiative forcing ($\Delta R_{[\text{CO}_2]}$) separately, we find a similar non-linearity in the $\Delta T_g - \Delta R_{[\text{CO}_2]}$ scatter plot only in the CO_2 data from ice cores (Fig. 7a). The relationship between temperature and radiative forcing of CO_2 are best described by a linear function in the Hönisch and Pagani data sets (Fig. 7c and g, Table 1) or in data from the Foster-lab even by a sec-

State-dependency of the equilibrium climate sensitivity

P. Köhler et al.

Title Page

Abstract

Introduction

Conclusions

References

Tables

Figures



Back

Close

Full Screen / Esc

Printer-friendly Version

Interactive Discussion



State-dependency of the equilibrium climate sensitivity

P. Köhler et al.

Title Page

Abstract

Introduction

Conclusions

References

Tables

Figures



Back

Close

Full Screen / Esc

Printer-friendly Version

Interactive Discussion



ond order polynomial with inverse slope leading to a decline in $S_{[\text{CO}_2]}$ for rising $\Delta R_{[\text{CO}_2]}$ (Fig. 7e). This inverse slope obtained for the Foster data between ΔT_g and $\Delta R_{[\text{CO}_2]}$ is the only case in which a detected nonlinearity partly depends on the use of the temperature change time series, e.g. the relationship is linear when based on ΔT_{g3} (Table 1).

Furthermore, this inverse slope might be caused by the under-representation of data for negative radiative forcing. However, when data in the ΔT_g - $\Delta R_{[X]}$ -scatter plots are binned in x or y direction to overcome any uneven distribution of data no change in the significance of the non-linearities are observed. The data scatter is large and regression coefficients between $\Delta R_{[\text{CO}_2]}$ and ΔT_g for Foster ($r^2 = 0.42$) and Pagani ($r^2 = 0.03$) are small. This large scatter and weak quality of the fit in the Pagani data is probably caused by some difficulties in the alkenone-based proxy, e.g. size dependency, and variations in the degree of passive vs. active uptake of CO_2 by the alkenone-producing coccolithophorids (Bolton and Stoll, 2013). Furthermore, van de Wal et al. (2011) already showed that the relationship of CO_2 to temperature change during the last 20 Myr is opposite in sign for alkenone-based CO_2 than for other approaches.

The ice-albedo forcing $\Delta R_{[\text{LI}]}$ has in our simulation results a specific relationship to global temperature change. Here both a step function or linear change in the polar amplification factor f_{pa} lead to similar results (Fig. 6b). However, when not 3-D ice-sheet models (de Boer et al., 2014) as used here, but simpler approaches to calculate $\Delta R_{[\text{LI}]}$ are applied, e.g. based on 1-D ice-sheet models (de Boer et al., 2010), related to sea level (Hansen et al., 2008; Martínez-Botí et al., 2015), or based on global land ice area changes without considering their latitudinal changes in detail (Köhler et al., 2010; PALAEOSENS-Project Members, 2012; von der Heydt et al., 2014) the ΔT_g - $\Delta R_{[\text{LI}]}$ -relationship is more linear. The range of $\Delta R_{[\text{LI}]}$ proposed for the same range of ΔT_g is then reduced by 30 % (Fig. 6b and c). $\Delta R_{[\text{LI}]}$ is effected by ice-sheet area rather than ice sheet volume. 3-D ice-sheet models include this effect better than calculations based on 1-D ice sheet models or directly from sea level variations. This non-linearity between ice volume (or sea level) and ice area is supported by data and theory of the scaling of glaciers (Bahr, 1997; Bahr et al., 2015). In addition, latitudinal variation of

land-ice distribution affect the radiative forcing $\Delta R_{[LI]}$ in a non-linear way (Fig. 1), and thereby likely contributes to a state-dependency in the equilibrium climate sensitivity $S_{[CO_2,LI]}$.

3.3 Calculating the specific equilibrium climate sensitivity $S_{[CO_2,LI]}$

The non-linear regression of the $\Delta T_g - \Delta R_{[CO_2,LI]}$ scatter plot revealed that both the ice core CO_2 and the Hönisch-lab data contain a state-dependency in $S_{[CO_2,LI]}$. As explained in Sect. 2.4 we analyse for both data sets the mean and uncertainty in $S_{[CO_2,LI]}$ from probability density functions for different background climate states represented by $\Delta R_{[CO_2,LI]}$ based on the point-wise results (Fig. 8). For both the Pagani and Foster data sets the slopes of the linear regression lines in $\Delta T_g - \Delta R_{[CO_2,LI]}$ might in principle be used to calculate $S_{[CO_2,LI]}$, however both data sets have a rather large offset in the y direction (ΔT_g) (y interception is far away from the origin), that might bias these results. These offsets are nearly identical when calculations are based on the alternative global temperature changes ΔT_{g2} or ΔT_{g3} (Table 1). Note, that $S_{[CO_2,LI]}$ as calculated for each data point in Fig. 8 also contains 20 and 11 outsiders in the ice core and Hönisch data sets, respectively, that fall not in the most plausible range of $0.0-3.0 \text{ KW}^{-1} \text{ m}^2$. These outsiders are typically generated, when dividing smaller anomalies in ΔT_g and $\Delta R_{[CO_2,LI]}$ during interglacials, when already small uncertainties generate a large change in the ratio in $\Delta T_g \cdot \Delta R_{[CO_2,LI]}^{-1}$. They are neglected from further analysis.

$S_{[CO_2,LI]}$ based on the ice core and Hönisch-lab data falls rarely below $0.8 \text{ KW}^{-1} \text{ m}^2$ (Fig. 8). We distinguish in both data sets “cold” from “warm” conditions using the threshold of $\Delta R_{[CO_2,LI]} = -3.5 \text{ W m}^{-2}$ to make our results comparable to the piece-wise linear analysis of “warm” and “cold” periods in von der Heydt et al. (2014). For the ice core data of the last 0.8 Myr the $S_{[CO_2,LI]}$ is not normally distributed, but has a long tail towards higher values (Fig. 8c). However, this long tail is partially caused by data points with $\Delta R_{[CO_2,LI]}$ not far from 0 W m^{-2} , which are prone to high uncertainties. Only conditions during “cold” periods, representing glacial maxima, have a nearly Gaussian

State-dependency of the equilibrium climate sensitivity

P. Köhler et al.

[Title Page](#)[Abstract](#)[Introduction](#)[Conclusions](#)[References](#)[Tables](#)[Figures](#)[Back](#)[Close](#)[Full Screen / Esc](#)[Printer-friendly Version](#)[Interactive Discussion](#)

State-dependency of the equilibrium climate sensitivity

P. Köhler et al.

Title Page

Abstract

Introduction

Conclusions

References

Tables

Figures



Back

Close

Full Screen / Esc

Printer-friendly Version

Interactive Discussion



(Fig. 1b) the appearance of large NH land ice first happened around 2.82 MyrBP, also the time which has been suggested by Sarnthein (2013) for the onset of NH land ice and when Martínez-Botí et al. (2015) found a pronounced decline in CO_2 . Note, that the start of northern hemispheric glaciation in our 3-D ice-sheet simulations was first gradual and intensified around 2.7 Myr ago (Fig. 1b), in agreement with other studies (Raymo, 1994; Haug et al., 2005). We tested the Foster-lab data for any changes in the regression analysis, when the data set was split in two time windows, one with and one without NH ice sheets. We found significantly different relationships between temperature change and radiative forcing for most of the Pleistocene than for either an ice-free NH Pliocene (Foster-lab data 2.82–3.3 MyrBP) or all available Pliocene data (Foster-lab data 2.5–3.3 MyrBP) (Fig. 10). For the Pleistocene $\Delta T_g - \Delta R_{[\text{CO}_2, \text{LI}]}$ data are in themselves non-linear (thus $S_{[\text{CO}_2, \text{LI}]}$ is state dependent), and for the Pliocene the relationship seems to be linear (thus $S_{[\text{CO}_2, \text{LI}]}$ to be constant) over the time window. However, the fit through $\Delta T_g - \Delta R_{[\text{CO}_2, \text{LI}]}$ is of low quality ($r^2 = 0.04$ for 2.82–3.3 MyrBP and $r^2 = 0.23$ for 2.5–3.3 MyrBP) which prevents us from calculating any quantitative values of $S_{[\text{CO}_2, \text{LI}]}$ based on them. Remember, that in all regression analyses we consider the uncertainties in both x and y direction in all data points by the application of Monte-Carlo statistics, something which also distinguishes our approach from Martínez-Botí et al. (2015) and possibly contributes to different results.

Nevertheless, our data compilation clearly points to a regime shift in the climate system with different climate sensitivities before and after 2.82 MyrBP. From the available proxy-based data indicating CO_2 around 400 ppmv in large parts of the Pliocene, together with our simulated global temperature change of around 2 K and ice-sheet albedo forcing of about 0.5 W m^{-2} (Fig. 4) we can estimate that in the NH-ice free Pliocene $S_{[\text{CO}_2, \text{LI}]}$ was around $1 \text{ K W}^{-1} \text{ m}^2$, in agreement with Martínez-Botí et al. (2015). This is of similar size as our results for full glacial conditions of most of the Pleistocene, but smaller than during intermediate glaciated to interglacial conditions of the late Pleistocene. A possible reason could be that in the warm Pliocene the sea ice-albedo feedback might have been weaker or even absent (von der Heydt et al., 2014),

but some studies (Stevens and Bony, 2013; Fedorov et al., 2013) also suggest that processes are missing in state-of-the-art climate models. A recent study (Kirtland Turner, 2014) concluded that at the onset of the northern hemispheric glaciation a fundamental change in the interplay of the carbon cycle and the climate system occurred leading to a switch from in-phase glacial/interglacial changes in deep ocean $\delta^{18}\text{O}$ and $\delta^{13}\text{C}$ to anti-phase changes. If true such a change in the carbon cycle/climate system might also affect climate sensitivity.

4 Discussion

Martínez-Botí et al. (2015) recently analysed the ice core CO_2 and the new CO_2 data from the Foster-lab around the end of the Pliocene separately finding $S_{[\text{CO}_2, \text{LI}]}$ of 0.91 ± 0.10 and $1.01 \pm 0.19 \text{KW}^{-1} \text{m}^2$, respectively. Both results are within their uncertainties nearly indistinguishable, thus Martínez-Botí et al. (2015) concluded that $S_{[\text{CO}_2, \text{LI}]}$ is not state-dependent, since it did not change between Pliocene and Pleistocene. However, since they based the radiative forcing of land-ice albedo ($\Delta R_{[\text{LI}]}$) on a linear function of sea level they miss an important non-linearity of the climate system. We find that the large uncertainty in $\Delta R_{[\text{CO}_2]}$ might also be another reason for state-independency in $S_{[\text{CO}_2, \text{LI}]}$ in the Foster-lab data set. $S_{[\text{CO}_2, \text{LI}]}$ based on the ice core analysis of Martínez-Botí et al. (2015) is slightly smaller than our results based on the cold periods from the ice core data set (Fig. 9). This indicates that the information, which are relevant to suggest any state dependency in $S_{[\text{CO}_2, \text{LI}]}$ are mainly contained in data covering the so-called “warm” climates of the Pleistocene. Thus, especially the land-ice area distribution and $\Delta R_{[\text{LI}]}$ from intermediate glaciated states are important here.

Comparing data-based estimates of $S_{[\text{CO}_2, \text{LI}]}$ directly with climate model results (e.g. Lunt et al., 2010) is not straightforward and in the following not performed, because in climate models only those processes considered explicitly as forcing will have an impact on calculated temperature change, while the data-based temperature reconstruction contains the effect of all processes (PALAEOSSENS-Project Members, 2012).

State-dependency of the equilibrium climate sensitivity

P. Köhler et al.

Title Page

Abstract

Introduction

Conclusions

References

Tables

Figures



Back

Close

Full Screen / Esc

Printer-friendly Version

Interactive Discussion



ing to our results, major implications for the expected equilibrium temperature rise. For projected future greenhouse gas emissions the Greenland ice sheet might completely disappear (Levermann et al., 2013) on the long-term, but it is projected to reduce its ice volume in the next two thousand years by less than 50%. This suggests that for the coming millennia the Earth still contains a significant amount of northern hemispheric land ice and thus climate and the proposed climate sensitivity $S_{[\text{CO}_2, \text{LI}]}$ are probably more comparable to interglacials of the late Pleistocene, before the system switches in the more distant future towards an ice-free Northern Hemisphere more comparable to the warm Pliocene.

5 Conclusions

In conclusion, we find that the specific equilibrium climate sensitivity based on radiative forcing of CO_2 and land ice albedo, $S_{[\text{CO}_2, \text{LI}]}$, is state-dependent, if CO_2 data from ice cores or from the Hönisch-lab, based on $\delta^{11}\text{B}$, are analysed. The state-dependency arises from the non-linear relationship between changes in radiative forcing of land ice albedo, $\Delta R_{[\text{LI}]}$, and changes in global temperature. Previous studies were not able to detect such a state-dependency because land ice albedo forcing was not based on results from 3-D ice-sheet models which contain much of this non-linearity. So far, the state-dependency of $S_{[\text{CO}_2, \text{LI}]}$ based on ice core CO_2 , which was derived from predominately glacial conditions of the late Pleistocene, can be extrapolated to the last 2.1 Myr. During intermediate glaciated and interglacial periods of most of the Pleistocene $S_{[\text{CO}_2, \text{LI}]}$ was on average by about $\sim 45\%$ higher (mean: $1.54 \text{KW}^{-1} \text{m}^2$; 68% probability range: $1.0\text{--}2.2 \text{KW}^{-1} \text{m}^2$) than during full glacial conditions of the Pleistocene (mean $1.06 \text{KW}^{-1} \text{m}^2$; 68% probability range: $0.8\text{--}1.4 \text{KW}^{-1} \text{m}^2$). Data uncertainties for the Pliocene do not allow a statistically well-supported conclusion on the value of $S_{[\text{CO}_2, \text{LI}]}$. The data available so far suggest that the appearance of northern hemispheric land-ice sheets changed the climate system and accordingly influenced

State-dependency of the equilibrium climate sensitivity

P. Köhler et al.

Title Page

Abstract

Introduction

Conclusions

References

Tables

Figures



Back

Close

Full Screen / Esc

Printer-friendly Version

Interactive Discussion



climate sensitivity. In the Pliocene $S_{[CO_2,LI]}$ was therefore probably smaller than during interglacials of the Pleistocene.

Acknowledgements. PMIP3 model output was derived from the LGM scenarios of CMIP5, PlioMIP model out from uploaded results published of its large scale features (Haywood et al., 2013). We acknowledge the World Climate Research Programme's Working Group on Coupled Modelling, which is responsible for CMIP. For CMIP the US Department of Energy's Program for Climate Model Diagnosis and Intercomparison provides coordinating support and led development of software infrastructure in partnership with the Global Organization for Earth System Science Portals. We thank the climate modeling groups from which we took results from both PMIP3 and PlioMIP as available mid January 2014 and as listed in the Methods Section of this paper for producing and making available their model output. We also thank G. Foster for providing CO₂ data and comments on our manuscript, B. Hönisch for insights to the measurements of the Bartoli data set and G. Knorr and J. Bijma for helpful comments. Financial support for B. de Boer was partially provided through the NWO-VICI grant of L. J. Lourens. L. Stap was funded by NWO-ALW. This paper contributes to the program of the Netherlands Earth System Science Centre (NESSC), financially supported by the Ministry of Education, Culture and Science (OCW). Data sets of ΔT_g and $\Delta R_{[LI]}$ will be available from www.pangaea.de.

References

- Abe-Ouchi, A., Segawa, T., and Saito, F.: Climatic Conditions for modelling the Northern Hemisphere ice sheets throughout the ice age cycle, *Clim. Past*, 3, 423–438, doi:10.5194/cp-3-423-2007, 2007. 3026
- Ahn, J. and Brook, E. J.: Siple Dome ice reveals two modes of millennial CO₂ change during the last ice age, *Nature Communications*, 5, 3723, doi:10.1038/ncomms4723, 2014. 3029, 3060
- Allen, K. A., Hönisch, B., Eggins, S. M., and Rosenthal, Y.: Environmental controls on B/Ca in calcite tests of the tropical planktic foraminifer species *Globigerinoides ruber* and *Globigerinoides sacculifer*, *Earth Planet. Sc. Lett.*, 351–352, 270–280, doi:10.1016/j.epsl.2012.07.004, 2012. 3030

State-dependency of the equilibrium climate sensitivity

P. Köhler et al.

Title Page

Abstract

Introduction

Conclusions

References

Tables

Figures



Back

Close

Full Screen / Esc

Printer-friendly Version

Interactive Discussion



**State-dependency of
the equilibrium
climate sensitivity**

P. Köhler et al.

[Title Page](#)[Abstract](#)[Introduction](#)[Conclusions](#)[References](#)[Tables](#)[Figures](#)[Back](#)[Close](#)[Full Screen / Esc](#)[Printer-friendly Version](#)[Interactive Discussion](#)

- Annan, J. D. and Hargreaves, J. C.: A new global reconstruction of temperature changes at the Last Glacial Maximum, *Clim. Past*, 9, 367–376, doi:10.5194/cp-9-367-2013, 2013. 3026, 3027, 3041
- Badger, M. P. S., Schmidt, D. N., Mackensen, A., and Pancost, R. D.: High-resolution alkenone palaeobarometry indicates relatively stable $p\text{CO}_2$ during the Pliocene (3.3–2.8 Ma), *Philos. T. R. Soc. A*, 371, doi:10.1098/rsta.2013.0094, 2013. 3030
- Bahr, D. B.: Global distributions of glacier properties: a stochastic scaling paradigm, *Water Resour. Res.*, 33, 1669–1679, doi:10.1029/97WR00824, 1997. 3036
- Bahr, D. B., Pfeffer, W. T., and Kaser, G.: A review of volume-area scaling of glaciers, *Rev. Geophys.*, 53, 95–140, doi:10.1002/2014RG000470, 2015. 3036
- Bartoli, G., Hönisch, B., and Zeebe, R. E.: Atmospheric CO_2 decline during the Pliocene intensification of Northern Hemisphere glaciations, *Paleoceanography*, 26, PA4213, doi:10.1029/2010PA002055, 2011. 3030
- Beerling, D. J. and Royer, D. L.: Convergent Cenozoic CO_2 history, *Nat. Geosci.*, 4, 418–420, doi:10.1038/ngeo1186, 2011. 3028
- Bereiter, B., Lüthi, D., Siegrist, M., Schüpbach, S., Stocker, T. F., and Fischer, H.: Mode change of millennial CO_2 variability during the last glacial cycle associated with a bipolar marine carbon seesaw, *P. Natl. Acad. Sci. USA*, 109, 9755–9760, doi:10.1073/pnas.1204069109, 2012. 3029, 3060
- Bereiter, B., Eggleston, S., Schmitt, J., Nehrbass-Ahles, C., Stocker, T. F., Fischer, H., Kipftuhl, S., and Chappellaz, J.: Revision of the EPICA Dome C CO_2 record from 800 to 600 kyr before present, *Geophys. Res. Lett.*, 42, 542–549, doi:10.1002/2014GL061957, 2015. 3028, 3029, 3060, 3062, 3066
- Bolton, C. T. and Stoll, H. M.: Late Miocene threshold response of marine algae to carbon dioxide limitation, *Nature*, 500, 558–562, doi:10.1038/nature12448, 2013. 3036
- Braconnot, P., Harrison, S. P., Kageyama, M., Bartlein, P. J., Masson-Delmotte, V., Abe-Ouchi, A., Otto-Bliesner, B., and Zhao, Y.: Evaluation of climate models using palaeoclimatic data, *Nature Climate Change*, 2, 417–424, doi:10.1038/nclimate1456, 2012. 3026
- Caballero, R. and Huber, M.: State-dependent climate sensitivity in past warm climates and its implications for future climate projections, *P. Natl. Acad. Sci. USA*, 110, 14162–14167, doi:10.1073/pnas.1303365110, 2013. 3022, 3023
- Crucifix, M.: Does the Last Glacial Maximum constrain climate sensitivity?, *Geophys. Res. Lett.*, 33, L18701, doi:10.1029/2006GL027137, 2006. 3022, 3023

State-dependency of the equilibrium climate sensitivity

P. Köhler et al.

Title Page

Abstract

Introduction

Conclusions

References

Tables

Figures



Back

Close

Full Screen / Esc

Printer-friendly Version

Interactive Discussion



de Boer, B., van de Wal, R. S. W., Bintanja, R., Lourens, L. J., and Tuentler, E.: Cenozoic global ice volume and temperature simulations with 1-D ice-sheet models forced by $\delta^{18}\text{O}$ records, *Ann. Glaciol.*, 51, 23–33, doi:10.3189/172756410791392736, 2010. 3036, 3064

de Boer, B., Lourens, L. J., and van de Wal, R. S.: Persistent 400,000-year variability of Antarctic ice volume and the carbon cycle is revealed throughout the Plio–Pleistocene, *Nature Communications*, 5, 2999, doi:10.1038/ncomms3999, 2014. 3024, 3025, 3027, 3028, 3032, 3033, 3036, 3056, 3058, 3063, 3064

de Boer, B., Dolan, A. M., Bernales, J., Gasson, E., Goelzer, H., Golledge, N. R., Sutter, J., Huybrechts, P., Lohmann, G., Rogozhina, I., Abe-Ouchi, A., Saito, F., and van de Wal, R. S. W.: Simulating the Antarctic ice sheet in the late-Pliocene warm period: PLISMIP-ANT, an ice-sheet model intercomparison project, *The Cryosphere*, 9, 881–903, doi:10.5194/tc-9-881-2015, 2015. 3041

Dolan, A. M., Hunter, S. J., Hill, D. J., Haywood, A. M., Koenig, S. J., Otto-Bliesner, B. L., Abe-Ouchi, A., Bragg, F., Chan, W.-L., Chandler, M. A., Contoux, C., Jost, A., Kamae, Y., Lohmann, G., Lunt, D. J., Ramstein, G., Rosenbloom, N. A., Sohl, L., Stepanek, C., Ueda, H., Yan, Q., and Zhang, Z.: Using results from the PlioMIP ensemble to investigate the Greenland Ice Sheet during the mid-Pliocene Warm Period, *Clim. Past*, 11, 403–424, doi:10.5194/cp-11-403-2015, 2015. 3041

Fedorov, A. V., Brierley, C. M., Lawrence, K. T., Liu, Z., Dekens, P. S., and Ravelo, A. C.: Patterns and mechanisms of early Pliocene warmth, *Nature*, 496, 43–49, doi:10.1038/nature12003, 2013. 3040, 3041

Forster, P., Ramaswamy, V., Artaxo, P., Bernsten, T., Betts, R., Fahey, D., Haywood, J., Lean, J., Lowe, D., Myhre, G., Nganga, J., Prinn, R., Raga, G., Schulz, M., and Dorland, R. V.: Changes in atmospheric constituents and in radiative forcing, in: *Climate Change 2007: The Physical Science Basis. Contribution of Working Group I to the Fourth Assessment Report of the Intergovernmental Panel on Climate Change*, edited by: Solomon, S., Qin, D., Manning, M., Chen, Z., Marquis, M., Averyt, K. B., Tignor, M., and Miller, H. L., Cambridge University Press, Cambridge, UK and New York, NY, USA, 129–234, 2007. 3033

Foster, G. L.: Seawater pH, $p\text{CO}_2$ and $[\text{CO}_3^{2-}]$ variations in the Caribbean Sea over the last 130 kyr: a boron isotope and B/Ca study of planktic foraminifera, *Earth Planet. Sc. Lett.*, 271, 254–266, 2008. 3029, 3060, 3062, 3066

Goldner, A., Huber, M., and Caballero, R.: Does Antarctic glaciation cool the world?, *Clim. Past*, 9, 173–189, doi:10.5194/cp-9-173-2013, 2013. 3022

State-dependency of the equilibrium climate sensitivity

P. Köhler et al.

Title Page

Abstract

Introduction

Conclusions

References

Tables

Figures



Back

Close

Full Screen / Esc

Printer-friendly Version

Interactive Discussion



- Hansen, J., Sato, M., Kharecha, P., Beerling, D., Berner, R., Masson-Delmotte, V., Pagan, M., Raymo, M., Royer, D. L., and Zachos, J. C.: Target atmospheric CO₂: where should humanity aim?, *The Open Atmospheric Science Journal*, 2, 217–231, doi:10.2174/1874282300802010217, 2008. 3034, 3036, 3064
- 5 Hansen, J., Sato, M., Russell, G., and Kharecha, P.: Climate sensitivity, sea level and atmospheric carbon dioxide, *Philos. T. R. Soc. A*, 371, doi:10.1098/rsta.2012.0294, 2013. 3021
- Hargreaves, J. C., Abe-Ouchi, A., and Annan, J. D.: Linking glacial and future climates through an ensemble of GCM simulations, *Clim. Past*, 3, 77–87, doi:10.5194/cp-3-77-2007, 2007. 3022, 3023, 3026
- 10 Haug, G. H., Ganopolski, A., Sigman, D. M., Rosell-Mele, A., Swann, G. E. A., Tiedemann, R., Jaccard, S. L., Bollamnn, J., maslin, M. A., Leng, M. J., and Eglinton, G.: North Pacific seasonality and the glaciation of North America 2.7 million years ago, *Nature*, 433, 821–825, 2005. 3039
- Hays, J. D., Imbrie, J., and Shackelton, N. J.: Variations in the Earth's orbit: pacemaker of the ice ages, *Science*, 194, 1121–1132, 1976. 3021
- 15 Haywood, A. M., Dowsett, H. J., Otto-Bliesner, B., Chandler, M. A., Dolan, A. M., Hill, D. J., Lunt, D. J., Robinson, M. M., Rosenbloom, N., Salzmann, U., and Sohl, L. E.: Pliocene Model Intercomparison Project (PlioMIP): experimental design and boundary conditions (Experiment 1), *Geosci. Model Dev.*, 3, 227–242, doi:10.5194/gmd-3-227-2010, 2010. 3023
- 20 Haywood, A. M., Hill, D. J., Dolan, A. M., Otto-Bliesner, B. L., Bragg, F., Chan, W.-L., Chandler, M. A., Contoux, C., Dowsett, H. J., Jost, A., Kamae, Y., Lohmann, G., Lunt, D. J., Abe-Ouchi, A., Pickering, S. J., Ramstein, G., Rosenbloom, N. A., Salzmann, U., Sohl, L., Stepanek, C., Ueda, H., Yan, Q., and Zhang, Z.: Large-scale features of Pliocene climate: results from the Pliocene Model Intercomparison Project, *Clim. Past*, 9, 191–209, doi:10.5194/cp-9-191-2013, 2013. 3024, 3026, 3044, 3058
- 25 Herbert, T. D., Peterson, L. C., Lawrence, K. T., and Liu, Z.: Tropical Ocean temperatures over the past 3.5 million years, *Science*, 328, 1530–1534, doi:10.1126/science.1185435, 2010. 3028
- Hönisch, B., Hemming, N. G., Archer, D., Siddall, M., and McManus, J. F.: Atmospheric carbon dioxide concentration across the Mid-Pleistocene Transition, *Science*, 324, 1551–1554, doi:10.1126/science.1171477, 2009. 3029, 3030, 3060, 3062, 3066, 3069
- 30 Kirtland Turner, S.: Pliocene switch in orbital-scale carbon cycle/climate dynamics, *Paleoceanography*, 29, 1256–1266, doi:10.1002/2014PA002651, 2014. 3040

State-dependency of the equilibrium climate sensitivity

P. Köhler et al.

Title Page

Abstract

Introduction

Conclusions

References

Tables

Figures



Back

Close

Full Screen / Esc

Printer-friendly Version

Interactive Discussion



- Koenig, S. J., Dolan, A. M., de Boer, B., Stone, E. J., Hill, D. J., DeConto, R. M., Abe-Ouchi, A., Lunt, D. J., Pollard, D., Quiquet, A., Saito, F., Savage, J., and van de Wal, R.: Ice sheet model dependency of the simulated Greenland Ice Sheet in the mid-Pliocene, *Clim. Past*, 11, 369–381, doi:10.5194/cp-11-369-2015, 2015. 3041
- 5 Köhler, P., Bintanja, R., Fischer, H., Joos, F., Knutti, R., Lohmann, G., and Masson-Delmotte, V.: What caused Earth's temperature variations during the last 800,000 years? Data-based evidences on radiative forcing and constraints on climate sensitivity, *Quaternary Sci. Rev.*, 29, 129–145, doi:10.1016/j.quascirev.2009.09.026, 2010. 3022, 3024, 3025, 3032, 3034, 3036, 3042
- 10 Kopp, G. and Lean, J. L.: A new, lower value of total solar irradiance: evidence and climate significance, *Geophys. Res. Lett.*, 38, L01706, doi:10.1029/2010GL045777, 2011. 3025
- Kutzbach, J. E., He, F., Vavrus, S. J., and Ruddiman, W. F.: The dependence of equilibrium climate sensitivity on climate state: applications to studies of climates colder than present, *Geophys. Res. Lett.*, 40, 3721–3726, doi:10.1002/grl.50724, 2013. 3022, 3023
- 15 Laskar, J., Robutel, P., Joutel, F., Gastineau, M., Correia, A. C. M., and Levrard, B.: A long term numerical solution for the insolation quantities of the Earth, *Astron. Astrophys.*, 428, 261–285, doi:10.1051/0004-6361:20041335, 2004. 3021, 3025, 3034, 3056, 3063
- Lawrence, K. T., Herbert, T. D., Brown, C. M., Raymo, M. E., and Haywood, A. M.: High-amplitude variations in North Atlantic sea surface temperature during the early Pliocene warm period, *Paleoceanography*, 24, PA2218, doi:10.1029/2008PA001669, 2009. 3028
- 20 Levermann, A., Clark, P. U., Marzeion, B., Milne, G. A., Pollard, D., Radic, V., and Robinson, A.: The multimillennial sea-level commitment of global warming, *P. Natl. Acad. Sci. USA*, 110, 13745–13750, doi:10.1073/pnas.1219414110, 2013. 3043
- Lisiecki, L. E. and Raymo, M. E.: A Pliocene–Pleistocene stack of 57 globally distributed benthic $\delta^{18}\text{O}$ records, *Paleoceanography*, 20, PA1003, doi:10.1029/2004PA001071, 2005. 3024, 3058
- 25 Lunt, D. J., Haywood, A. M., Schmidt, G. A., Salzmann, U., Valdes, P. J., and Dowsett, H. J.: Earth system sensitivity inferred from Pliocene modelling and data, *Nat. Geosci.*, 3, 60–64, doi:10.1038/ngeo706, 2010. 3040
- 30 MacFarling-Meure, C., Etheridge, D., Trudinger, C., Langenfelds, R., van Ommen, T., Smith, A., and Elkins, J.: Law Dome CO_2 , CH_4 and N_2O ice core records extended to 2000 years BP, *Geophys. Res. Lett.*, 33, L14810, doi:10.1029/2006GL026152, 2006. 3028, 3060

State-dependency of the equilibrium climate sensitivity

P. Köhler et al.

[Title Page](#)

[Abstract](#)

[Introduction](#)

[Conclusions](#)

[References](#)

[Tables](#)

[Figures](#)



[Back](#)

[Close](#)

[Full Screen / Esc](#)

[Printer-friendly Version](#)

[Interactive Discussion](#)



- Marcott, S. A., Bauska, T. K., Buizert, C., Steig, E. J., Rosen, J. L., Cuffey, K. M., Fudge, T. J., Severinghaus, J. P., Ahn, J., Kalk, M. L., McConnell, J. R., Sowers, T., Taylor, K. C., White, J. W., and Brook, E. J.: Centennial scale changes in the global carbon cycle during the last deglaciation, *Nature*, 514, 616–619, doi:10.1038/nature13799, 2014. 3029, 3060
- 5 Martínez-Botí, M. A., Foster, G. L., Chalk, T. B., Rohling, E. J., Sexton, P. F., Lunt, D. J., Pancost, R. D., Badger, M. P. S., and Schmidt, D. N.: Plio–Pleistocene climate sensitivity evaluated using high-resolution CO₂ records, *Nature*, 518, 49–54, doi:10.1038/nature14145, 2015. 3023, 3029, 3030, 3034, 3036, 3039, 3040, 3060, 3062, 3064, 3066, 3068, 3069
- Martínez-García, A., Rosell-Melé, A., McClymont, E. L., Gersonde, R., and Haug, G. H.: Sub-polar link to the emergence of the modern equatorial Pacific cold tongue, *Science*, 328, 1550–1553, doi:10.1126/science.1184480, 2010. 3028
- 10 Masson-Delmotte, V., Kageyama, M., Braconnot, P., Charbit, S., Krinner, G., Ritz, C., Guilyardi, E., Jouzel, J., Abe-Ouchi, A., Cruci, M., Gladstone, R. M., Hewitt, C. D., Kitoh, A., LeGrande, A. N., Marti, O., Merkel, U., Ohgaito, T. M. R., Otto-Bliesner, B., Peltier, W. R., Ross, I., Valdes, P. J., Vettoretti, G., Weber, S. L., Wolk, F., and YU, Y.: Past and future polar amplification of climate change: climate model intercomparisons and ice-core constraints, *Clim. Dynam.*, 26, 513–529, 2006. 3026
- 15 Meraner, K., Mauritsen, T., and Voigt, A.: Robust increase in equilibrium climate sensitivity under global warming, *Geophys. Res. Lett.*, 40, 5944–5948, doi:10.1002/2013GL058118, 2013. 3022, 3023
- 20 Milankovitch, M.: Kanon der Erdbestrahlung und seine Anwendung auf das Eiszeitenproblem, Special Publications Vol. 132, vol. 33 of Section Mathematics and Natural Sciences, Royal Serbian Academy, Belgrad, 1941. 3021
- Monnin, E., Indermühle, A., Dällenbach, A., Flückiger, J., Stauffer, B., Stocker, T. F., Raynaud, D., and Barnola, J.-M.: Atmospheric CO₂ concentrations over the last glacial termination, *Science*, 291, 112–114, doi:10.1126/science.291.5501.112, 2001. 3028, 3060
- 25 Monnin, E., Steig, E. J., Siegenthaler, U., Kawamura, K., Schwander, J., Stauffer, B., Stocker, T. F., Morse, D. L., Barnola, J.-M., Bellier, B., Raynaud, D., and Fischer, H.: Evidence for substantial accumulation rate variability in Antarctica during the Holocene, through synchronization of CO₂ in the Taylor Dome, Dome C and DML ice cores, *Earth Planet. Sc. Lett.*, 224, 45–54, 2004. 3028, 3060
- 30 Myhre, G., Highwood, E. J., Shine, K. P., and Stordal, F.: New estimates of radiative forcing due to well mixed greenhouse gases, *Geophys. Res. Lett.*, 25, 2715–2718, 1998. 3030

State-dependency of the equilibrium climate sensitivity

P. Köhler et al.

Title Page

Abstract

Introduction

Conclusions

References

Tables

Figures



Back

Close

Full Screen / Esc

Printer-friendly Version

Interactive Discussion



Nowack, P. J., Luke Abraham, N., Maycock, A. C., Braesicke, P., Gregory, J. M., Joshi, M. M., Osprey, A., and Pyle, J. A.: A large ozone-circulation feedback and its implications for global warming assessments, *Nature Climate Change*, 5, 41–45, doi:10.1038/nclimate2451, 2015. 3021

5 Pagani, M., Liu, Z., LaRiviere, J., and Ravelo, A. C.: High Earth-system climate sensitivity determined from Pliocene carbon dioxide concentrations, *Nat. Geosci.*, 3, 27–30, doi:10.1038/ngeo724, 2010. 3029, 3060, 3062, 3066

PALAEOSSENS-Project Members: Making sense of palaeoclimate sensitivity, *Nature*, 491, 683–691, doi:10.1038/nature11574, 2012. 3021, 3022, 3030, 3036, 3040, 3041, 3042

10 Peltier, W. R.: Global glacial isostasy and the surface of the ice-age Earth: the ICE-5G (VM2) model and GRACE, *Annu. Rev. Earth Pl. Sc.*, 32, 111–149, doi:10.1146/annurev.earth.32.082503.144359, 2004. 3026, 3034, 3063, 3064

Peltier, W. R., Argus, D. F., and Drummond, R.: Space geodesy constrains ice age terminal deglaciation: the global ICE-6G_C (VM5a) model, *J. Geophys. Res.-Sol. Ea.*, 120, 450–487, doi:10.1002/2014JB011176, 2015. 3026

15 Petit, J. R., Jouzel, J., Raynaud, D., Barkov, N. I., Barnola, J.-M., Basile, I., Bender, M., Chappellaz, J., Davis, M., Delaygue, G., Delmotte, M., Kotlyakov, V. M., Legrand, M., Lipenkov, V. Y., Lorius, C., Pépin, L., Ritz, C., Saltzman, E., and Stievenard, M.: Climate and atmospheric history of the past 420,000 years from the Vostok ice core, *Antarctica, Nature*, 399, 429–436, 1999. 3029, 3060

Press, W. H., Teukolsky, S. A., Vetterling, W. T., and Flannery, B. P.: *Numerical Recipes in Fortran*, second edition, Cambridge University Press, Cambridge, 1992. 3032

Raymo, M. E.: The initiation of Northern Hemisphere glaciation, *Annu. Rev. Earth Pl. Sc.*, 22, 353–383, 1994. 3039

25 Rohling, E. J., Foster, G. L., Grant, K. M., Marino, G., Roberts, A. P., Tamisiea, M. E., and Williams, F.: Sea-level and deep-sea-temperature variability over the past 5.3 million years, *Nature*, 508, 477–482, doi:10.1038/nature13230, 2014. 3041

Roth, R. and Joos, F.: A reconstruction of radiocarbon production and total solar irradiance from the Holocene ^{14}C and CO_2 records: implications of data and model uncertainties, *Clim. Past*, 9, 1879–1909, doi:10.5194/cp-9-1879-2013, 2013. 3025

30 Rovere, A., Raymo, M., Mitrovica, J., Hearty, P., O’Leary, M., and Inglis, J.: The Mid-Pliocene sea-level conundrum: Glacial isostasy, eustasy and dynamic topography, *Earth Planet. Sc. Lett.*, 387, 27–33, doi:10.1016/j.epsl.2013.10.030, 2014. 3041

State-dependency of the equilibrium climate sensitivity

P. Köhler et al.

[Title Page](#)[Abstract](#)[Introduction](#)[Conclusions](#)[References](#)[Tables](#)[Figures](#)[Back](#)[Close](#)[Full Screen / Esc](#)[Printer-friendly Version](#)[Interactive Discussion](#)

- Rubino, M., Etheridge, D. M., Trudinger, C. M., Allison, C. E., Battle, M. O., Langenfelds, R. L., Steele, L. P., Curran, M., Bender, M., White, J. W. C., Jenk, T. M., Blunier, T., and Francey, R. J.: A revised 1000-year atmospheric $\delta^{13}\text{C-CO}_2$ record from Law Dome and South Pole, Antarctica, *J. Geophys. Res.-Atmos.*, 118, 8482–8499, doi:10.1002/jgrd.50668, 2013. 3028, 3060
- 5 Sarnthein, M.: Transition from late Neogene to early Quaternary environments, in: *The Encyclopedia of Quaternary Science*, vol. 2, edited by: Elias, S., Elsevier, Amsterdam, 151–166, 2013. 3039
- Schmidt, G. A., Annan, J. D., Bartlein, P. J., Cook, B. I., Guilyardi, E., Hargreaves, J. C., Harrison, S. P., Kageyama, M., LeGrande, A. N., Konecky, B., Lovejoy, S., Mann, M. E., Masson-Delmotte, V., Risi, C., Thompson, D., Timmermann, A., Tremblay, L.-B., and Yiou, P.: Using palaeo-climate comparisons to constrain future projections in CMIP5, *Clim. Past*, 10, 221–250, doi:10.5194/cp-10-221-2014, 2014. 3027, 3041
- 10 Schmidtner, A., Urban, N. M., Shakun, J. D., Mahowald, N. M., Clark, P. U., Bartlein, P. J., Mix, A. C., and Rosell-Melé, A.: Climate sensitivity estimated from temperature reconstructions of the Last Glacial Maximum, *Science*, 334, 1385–1388, doi:10.1126/science.1203513, 2011. 3041
- Schneider, R., Schmitt, J., Köhler, P., Joos, F., and Fischer, H.: A reconstruction of atmospheric carbon dioxide and its stable carbon isotopic composition from the penultimate glacial maximum to the last glacial inception, *Clim. Past*, 9, 2507–2523, doi:10.5194/cp-9-2507-2013, 2013. 3028, 3060
- 20 Seki, O., Foster, G. L., Schmidt, D. N., Mackensen, A., Kawamura, K., and Pancost, R. D.: Alkenone and boron-based Pliocene $p\text{CO}_2$ records, *Earth Planet. Sc. Lett.*, 292, 201–211, doi:10.1016/j.epsl.2010.01.037, 2010. 3030
- Shindell, D. T.: Inhomogeneous forcing and transient climate sensitivity, *Nature Climate Change*, 4, 274–277, doi:10.1038/nclimate2136, 2014. 3021, 3022, 3042
- Siegenthaler, U., Stocker, T. F., Monnin, E., Lüthi, D., Schwander, J., Stauffer, B., Raynaud, D., Barnola, J.-M., Fischer, H., Masson-Delmotte, V., and Jouzel, J.: Stable carbon cycle–climate relationship during the late Pleistocene, *Science*, 310, 1313–1317, doi:10.1126/science.1120130, 2005. 3028, 3060
- 30 Singarayer, J. S. and Valdes, P. J.: High-latitude climate sensitivity to ice-sheet forcing over the last 120 kyr, *Quaternary Sci. Rev.*, 29, 43–55, doi:10.1016/j.quascirev.2009.10.011, 2010. 3026

**State-dependency of
the equilibrium
climate sensitivity**

P. Köhler et al.

[Title Page](#)[Abstract](#)[Introduction](#)[Conclusions](#)[References](#)[Tables](#)[Figures](#)[Back](#)[Close](#)[Full Screen / Esc](#)[Printer-friendly Version](#)[Interactive Discussion](#)

- Stap, L. B., van de Wal, R. S. W., de Boer, B., Bintanja, R., and Lourens, L. J.: Interaction of ice sheets and climate during the past 800 000 years, *Clim. Past*, 10, 2135–2152, doi:10.5194/cp-10-2135-2014, 2014. 3026
- Stevens, B. and Bony, S.: What are climate models missing?, *Science*, 340, 1053–1054, doi:10.1126/science.1237554, 2013. 3040
- Stocker, T. F., Qin, D., Tignor, G.-K. P. M., Allen, S., Boschung, J., Nauels, A., Xia, Y., Bex, V., and Midgley, P. (Eds.): IPCC, 2013: Climate Change 2013: The Physical Science Basis. Contribution of Working Group I to the Fifth Assessment Report of the Intergovernmental Panel on Climate Change, Cambridge University Press, Cambridge, UK and New York, NY, USA, 2013. 3021, 3022, 3042
- Tripati, A. K., Roberts, C. D., and Eagle, R. A.: Coupling of CO₂ and ice sheet stability over major climate transitions of the last 20 million years, *Science*, 326, 1394–1397, doi:10.1126/science.1178296, 2009. 3030
- Unger, N. and Yue, X.: Strong chemistry-climate feedbacks in the Pliocene, *Geophys. Res. Lett.*, 41, 527–533, doi:10.1002/2013GL058773, 2014. 3041
- van de Wal, R. S. W., de Boer, B., Lourens, L. J., Köhler, P., and Bintanja, R.: Reconstruction of a continuous high-resolution CO₂ record over the past 20 million years, *Clim. Past*, 7, 1459–1469, doi:10.5194/cp-7-1459-2011, 2011. 3024, 3036, 3064
- Vial, J., Dufresne, J.-L., and Bony, S.: On the interpretation of inter-model spread in CMIP5 climate sensitivity estimates, *Clim. Dynam.*, 41, 3339–3362, doi:10.1007/s00382-013-1725-9, 2013. 3021
- von der Heydt, A. S., Köhler, P., van de Wal, R. S., and Dijkstra, H. A.: On the state dependency of fast feedback processes in (paleo) climate sensitivity, *Geophys. Res. Lett.*, 41, 6484–6492, doi:10.1002/2014GL061121, 2014. 3023, 3031, 3034, 3035, 3036, 3037, 3038, 3039, 3068
- Yoshimori, M., Yokohata, T., and Abe-Ouchi, A.: A comparison of climate feedback strength between CO₂ doubling and LGM experiments, *J. Climate*, 22, 3374–3395, doi:10.1175/2009JCLI2801.1, 2009. 3026
- Yoshimori, M., Hargreaves, J. C., Annan, J. D., Yokohata, T., and Abe-Ouchi, A.: Dependency of feedbacks on forcing and climate state in physics parameter ensembles, *J. Climate*, 24, 6440–6455, doi:10.1175/2011JCLI3954.1, 2011. 3022
- Zeebe, R. E.: Time-dependent climate sensitivity and the legacy of anthropogenic greenhouse gas emissions, *P. Natl. Acad. Sci. USA*, 110, 13739–13744, doi:10.1073/pnas.1222843110, 2013. 3021, 3042

Zhang, Y. G., Pagani, M., Liu, Z., Bohaty, S. M., and DeConto, R.: A 40-million-year history of atmospheric CO₂, Philos. T. R. Soc. A, 371, 20130096, doi:10.1098/rsta.2013.0096, 2013. 3029, 3060, 3062, 3066

Discussion Paper | Discussion Paper | Discussion Paper | Discussion Paper | Discussion Paper

CPD

11, 3019–3069, 2015

State-dependency of the equilibrium climate sensitivity

P. Köhler et al.

Title Page

Abstract

Introduction

Conclusions

References

Tables

Figures

◀

▶

◀

▶

Back

Close

Full Screen / Esc

Printer-friendly Version

Interactive Discussion



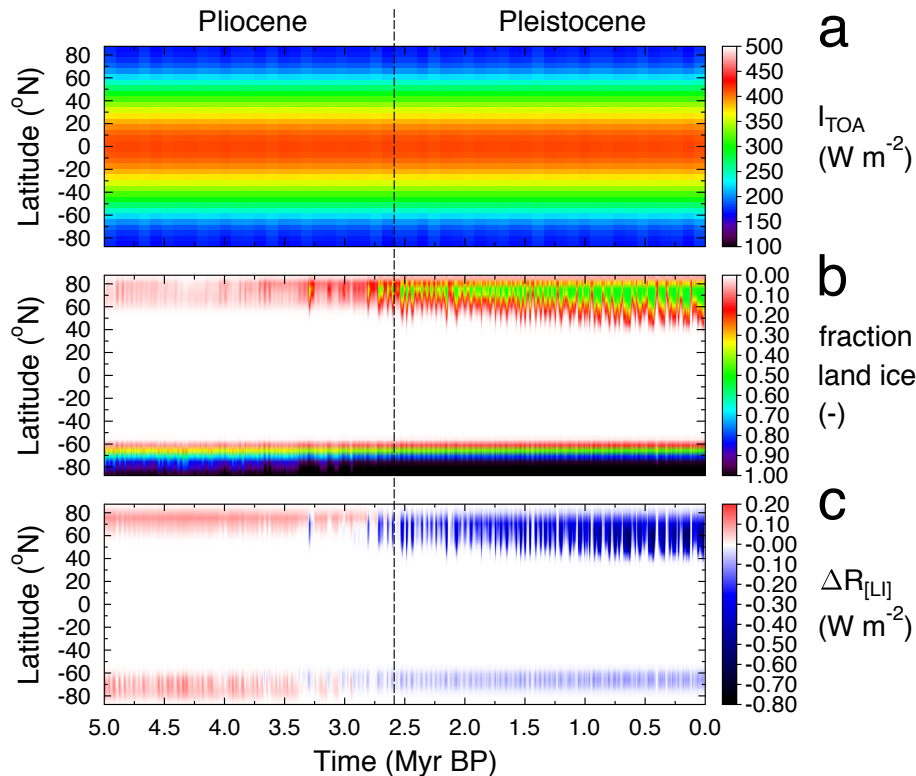
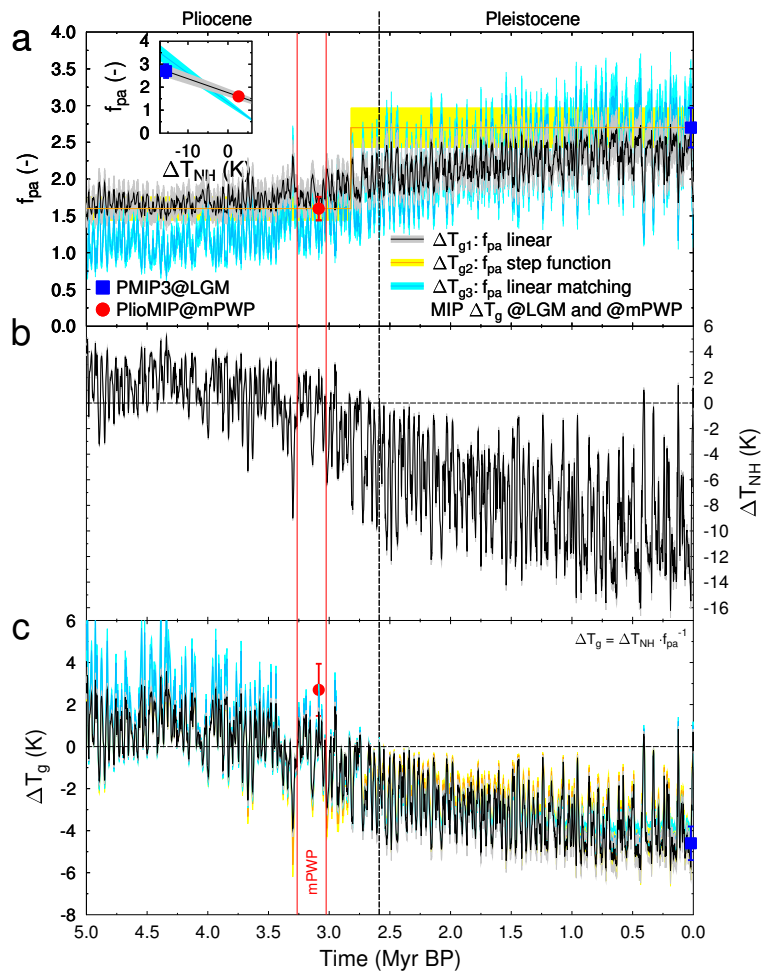


Figure 1. Radiative forcing of land ice sheets averaged for latitudinal bands of 5° . **(a)** Annual mean insolation at the top of the atmosphere I_{TOA} based on orbital variations (Laskar et al., 2004). **(b)** Fraction of each latitudinal bands of 5° covered by land ice as simulated by the 3-D ice-sheet model ANICE (de Boer et al., 2014). **(c)** Calculated radiative forcing of land ice sheets $\Delta R_{\text{[LI]}}$ normalised to global-scale impact.

State-dependency of the equilibrium climate sensitivity

P. Köhler et al.



[Title Page](#)

[Abstract](#) [Introduction](#)

[Conclusions](#) [References](#)

[Tables](#) [Figures](#)

[◀](#) [▶](#)

[◀](#) [▶](#)

[Back](#) [Close](#)

[Full Screen / Esc](#)

[Printer-friendly Version](#)

[Interactive Discussion](#)



Figure 2. Calculating global surface temperature change ΔT_g . **(a)** Polar amplification factor f_{pa} , the ratio between Northern Hemisphere (NH) land temperature change ΔT_{NH} and global temperature change ΔT_g , as function of time based on values for LGM (blue square) and mid-Pliocene Warm Period (mPWP) (red circle) derived from the Model Intercomparison Projects (MIP) PMIP3/CMIP5 and PlioMIP (Haywood et al., 2013), respectively. In our standard application ΔT_{g1} (black line) f_{pa} is calculated as a linear function depending on northern hemispheric temperature change ΔT_{NH} (insert), inter- and extrapolated between these two PMIP3 and PlioMIP-based values. Alternatively (ΔT_{g2} , orange line), f_{pa} varies as a step function with high values for the Pleistocene (periods with Northern Hemisphere land ice sheets) and low values for the Pliocene (periods mainly without NH land ice sheets) with the step between both values occurring at 2.82 MyrBP, when our results indicate large changes in NH land ice. In ΔT_{g3} (blue line) f_{pa} varied freely to meet ΔT_g reconstructed for LGM by PMIP3 (-4.6K) and for the mPWP by PlioMIP ($+2.7\text{K}$). See methods for further details. **(b)** NH temperature change ΔT_{NH} as deconvolved from the benthic $\delta^{18}\text{O}$ stack LR04 (Lisiecki and Raymo, 2005) by applying a 3-D ice-sheet model in an inverse mode (de Boer et al., 2014). Uncertainty in ΔT_{NH} (grey) is the 1σ error calculated from 8 different model realisations (de Boer et al., 2014). **(c)** Global surface temperature change ΔT_g as used here based on $\Delta T_g = \Delta T_{NH} \cdot f_{pa}^{-1}$. Results for ΔT_g based on all three approaches for f_{pa} are given (same colour code as in sub-figure **(a)**). Symbols show $\Delta T_g \pm 1\sigma$ as derived within PlioMIP (mPWP, red circle) and PMIP3/CMIP5 (LGM, blue square). Red vertical lines mark the time period of the mPWP.

State-dependency of the equilibrium climate sensitivity

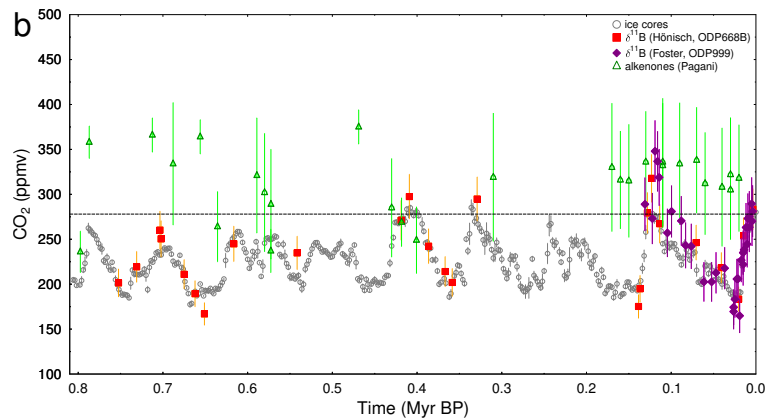
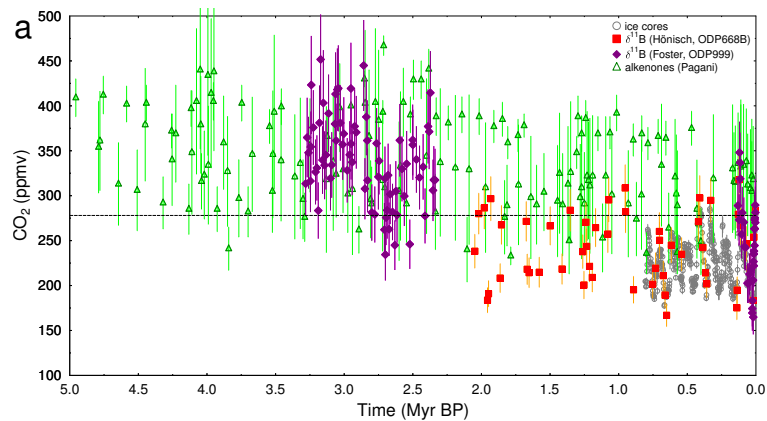
P. Köhler et al.

Title Page	
Abstract	Introduction
Conclusions	References
Tables	Figures
◀	▶
◀	▶
Back	Close
Full Screen / Esc	
Printer-friendly Version	
Interactive Discussion	



State-dependency of the equilibrium climate sensitivity

P. Köhler et al.



Title Page

Abstract

Introduction

Conclusions

References

Tables

Figures



Back

Close

Full Screen / Esc

Printer-friendly Version

Interactive Discussion



Figure 4. Changes in temperature and radiative forcing over the last 5 Myr. **(a)** Global mean surface temperature change ΔT_g calculated with the polar amplification factor f_{pa} being a linear function of the Northern Hemisphere land temperature change ΔT_{NH} . Marked are the mid-Pliocene Warm Period (mPWP) (red horizontal bar), global warming calculated within PlioMIP (red circle), and global cooling during the LGM derived from PMIP3/CMIP5 (blue square). **(b)** Changes in radiative forcing based on atmospheric CO_2 ($\Delta R_{[CO_2]}$). CO_2 data from ice cores (Bereiter et al., 2015) and based on $\delta^{11}B$ (Hönisch-lab (Hönisch et al., 2009), Foster-lab (Foster, 2008; Martínez-Botí et al., 2015)) and on alkenones (Pagani-lab (Pagani et al., 2010; Zhang et al., 2013)), **(c)** radiative forcing of land ice $\Delta R_{[L_i]}$ and for comparison global annual mean insolation changes due to orbital variation $\Delta R_{[orbit]}$. **(d)** The sum of the radiative forcing changes due to CO_2 and land ice sheets ($\Delta R_{[CO_2, L_i]}$) whenever CO_2 data allow its calculation. Uncertainties show 1σ .

State-dependency of the equilibrium climate sensitivity

P. Köhler et al.

Title Page	
Abstract	Introduction
Conclusions	References
Tables	Figures
◀	▶
◀	▶
Back	Close
Full Screen / Esc	
Printer-friendly Version	
Interactive Discussion	



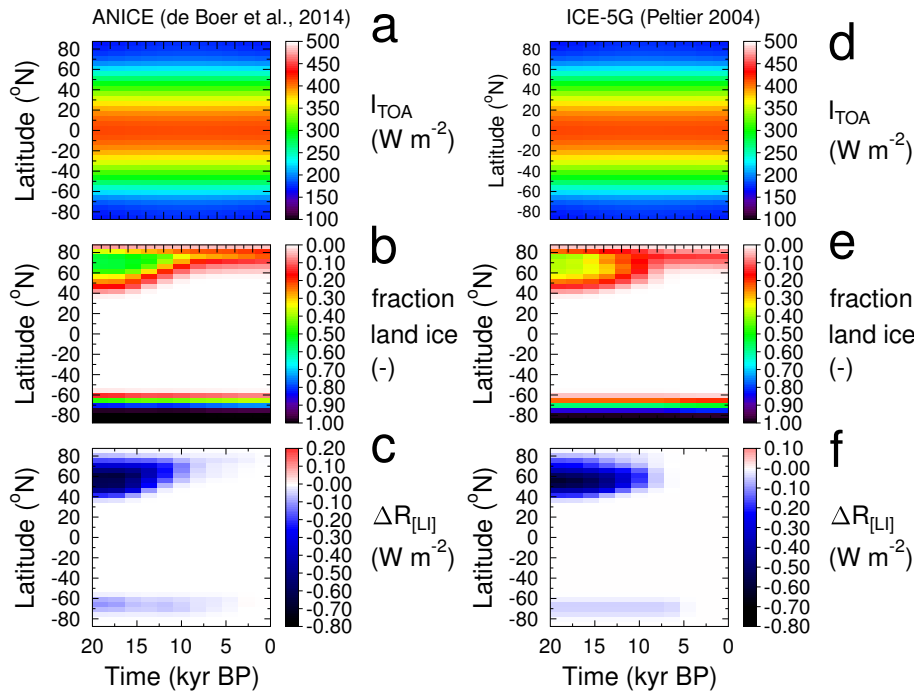


Figure 5. Comparing the calculation of radiative forcing of land ice sheets for the last 20 kyr for two different ice sheet setups. Left: the 3-D ice sheet model ANICE used in this study (de Boer et al., 2014); right: based on $1^\circ \times 1^\circ$ model output from ICE-5G (Peltier, 2004), results for radiative forcing of land ice sheets $\Delta R_{[LI]}$ is then based on similar aggregation to latitudinal bands of 5° as for ANICE. **(a, d)** Annual mean insolation at the top of the atmosphere I_{TOA} based on orbital variations (Laskar et al., 2004). **(b, e)** Fraction of each latitudinal bands of 5° covered by land ice as simulated by the 3-D ice-sheet models. **(c, f)** Calculated radiative forcing of land ice sheets $\Delta R_{[LI]}$ normalised to global-scale impact.

State-dependency of the equilibrium climate sensitivity

P. Köhler et al.

Title Page

Abstract

Introduction

Conclusions

References

Tables

Figures



Back

Close

Full Screen / Esc

Printer-friendly Version

Interactive Discussion

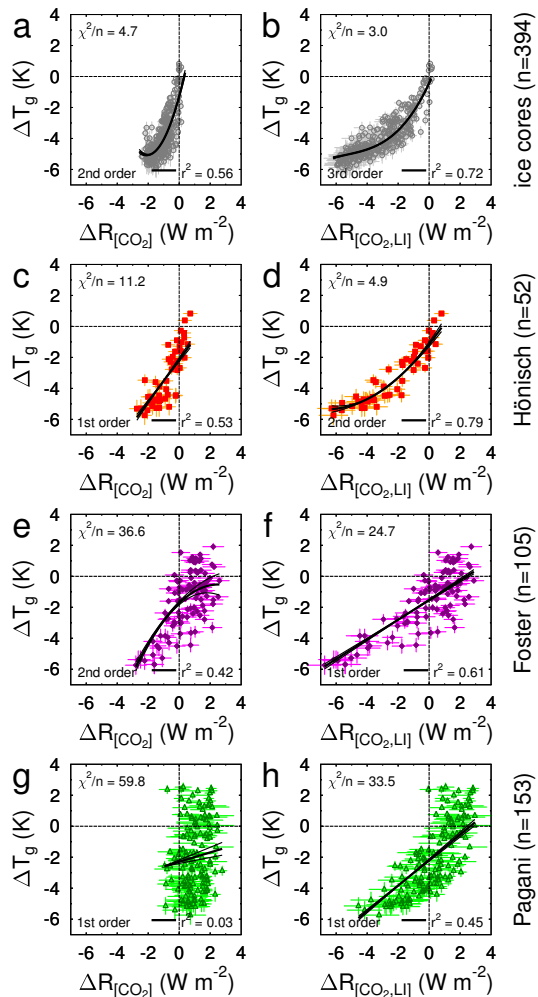


CPD

11, 3019–3069, 2015

State-dependency of the equilibrium climate sensitivity

P. Köhler et al.



Title Page

Abstract

Introduction

Conclusions

References

Tables

Figures



Back

Close

Full Screen / Esc

Printer-friendly Version

Interactive Discussion



Figure 7. Scatter-plots of data of global temperature change ΔT_g against radiative forcing $\Delta R_{[X]}$. ΔT_g is calculated with the polar amplification factor f_{pa} being a linear function of ΔT_{NH} . Left column **(a, c, e, g)**: radiative forcing of CO₂ ($\Delta R_{[CO_2]}$). Right column **(b, d, f, h)**: radiative forcing of CO₂ and land-ice albedo ($\Delta R_{[CO_2,LI]}$). Lines show average best fits (1st, 2nd, or 3rd order polynomials) to 5000 Monte-Carlo realisations of the data (details in Table 1). Sub-figures differ by the CO₂ data they are based on: **(a, b)** ice cores (Bereiter et al., 2015); **(c, d)** $\delta^{11}B$ from Hönisch-lab (Hönisch et al., 2009); **(e, f)** $\delta^{11}B$ from Foster-lab (Foster, 2008; Martínez-Botí et al., 2015); **(g, h)** alkenones from Pagani-lab (Pagani et al., 2010; Zhang et al., 2013); each row contains information on the number of data points n , each sub-figure the mean uncertainty of the fit by dividing χ^2 (the weighted sum of squares from the regression analysis) by n and the correlation coefficient r^2 . Uncertainties show 1σ .

State-dependency of the equilibrium climate sensitivity

P. Köhler et al.

Title Page	
Abstract	Introduction
Conclusions	References
Tables	Figures
◀	▶
◀	▶
Back	Close
Full Screen / Esc	
Printer-friendly Version	
Interactive Discussion	



State-dependency of the equilibrium climate sensitivity

P. Köhler et al.

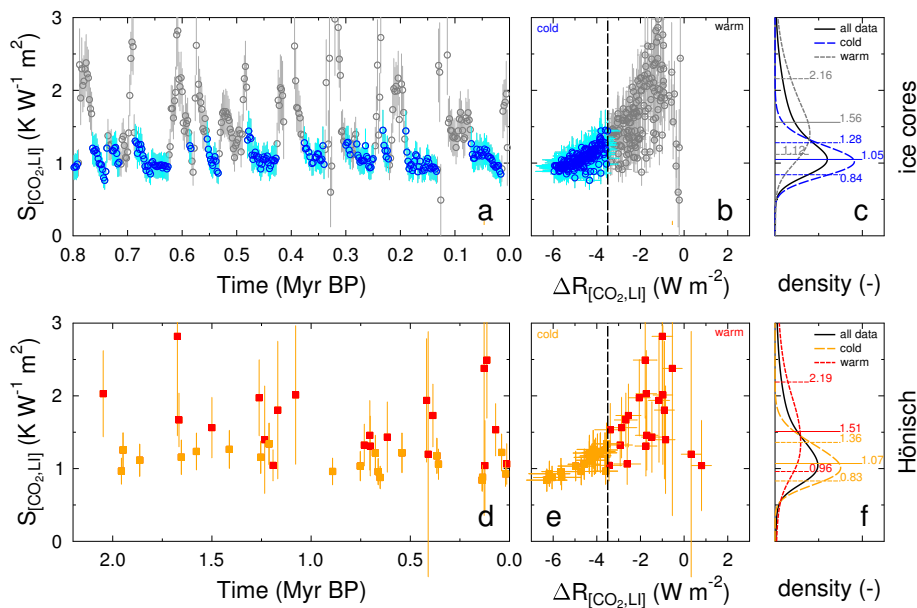


Figure 8. Calculating specific equilibrium climate sensitivity $S_{[CO_2,LI]}$. Only data with their mean in $S_{[CO_2,LI]}$ in the range $[0, 3] \text{KW}^{-1} \text{m}^2$ are analysed and plotted. **(a)** Ice core-based time series of point-wise calculations of $S_{[CO_2,LI]}$ for the last 0.8 Myr. **(b)** Same data as in **(a)** in a scatter plot of $S_{[CO_2,LI]}$ against radiative forcing $\Delta R_{[CO_2,LI]}$. **(c)** Probability density distribution of ice core-based $S_{[CO_2,LI]}$. Data from “cold” periods ($\Delta R_{[CO_2,LI]} < -3.5 \text{W m}^{-2}$) and “warm” periods ($\Delta R_{[CO_2,LI]} > -3.5 \text{W m}^{-2}$) are analysed separately. Labels in **(c)** denote 16th, 50th and 84th percentile. **(d, e, f)** Same as **(a, b, c)**, but for Hönisch data over the last 2.1 Myr.

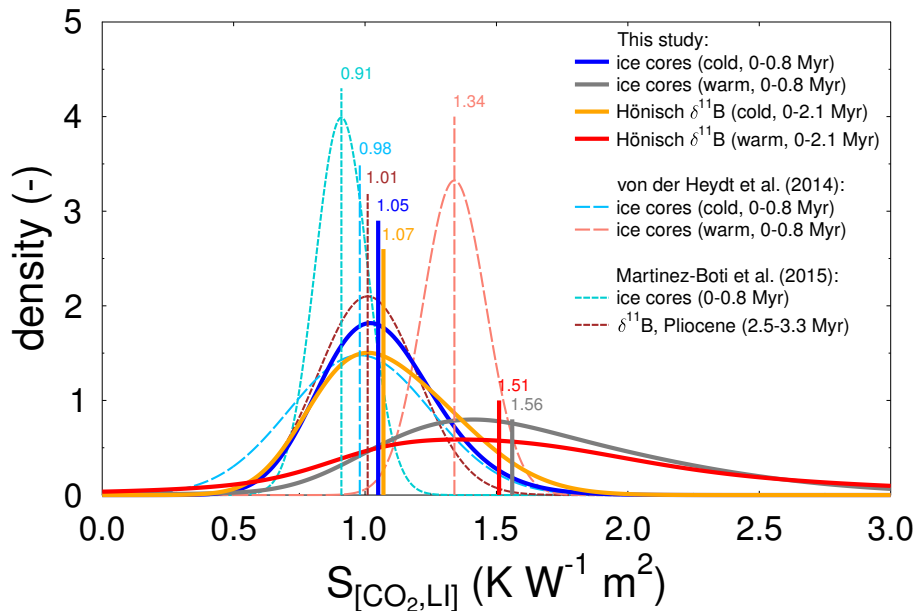


Figure 9. Probability density function of different approaches to calculate specific equilibrium climate sensitivity $S_{[CO_2,LI]}$. Results of this study are based on point-wise analysis of the ice core (last 0.8 Myr) and Hönisch (last 2.1 Myr) data for “cold” periods ($\Delta R_{[CO_2,LI]} < -3.5 W m^{-2}$) and “warm” periods ($\Delta R_{[CO_2,LI]} > -3.5 W m^{-2}$). von der Heydt et al. (2014) calculated $S_{[CO_2,LI]}$ based on ice core data for similar split of the data. We show their results based on similar ΔT_g than obtained here published in the SI in von der Heydt et al. (2014). Martínez-Botí et al. (2015) calculated $S_{[CO_2,LI]}$ for either ice core data of the whole last 0.8 Myr or based on $\delta^{11}B$ for 0.8 Myr of the Pliocene between 2.5–3.3 Myr BP. Vertical lines and labels give the mean of the different results.

State-dependency of the equilibrium climate sensitivity

P. Köhler et al.

Title Page

Abstract

Introduction

Conclusions

References

Tables

Figures



Back

Close

Full Screen / Esc

Printer-friendly Version

Interactive Discussion



State-dependency of the equilibrium climate sensitivity

P. Köhler et al.

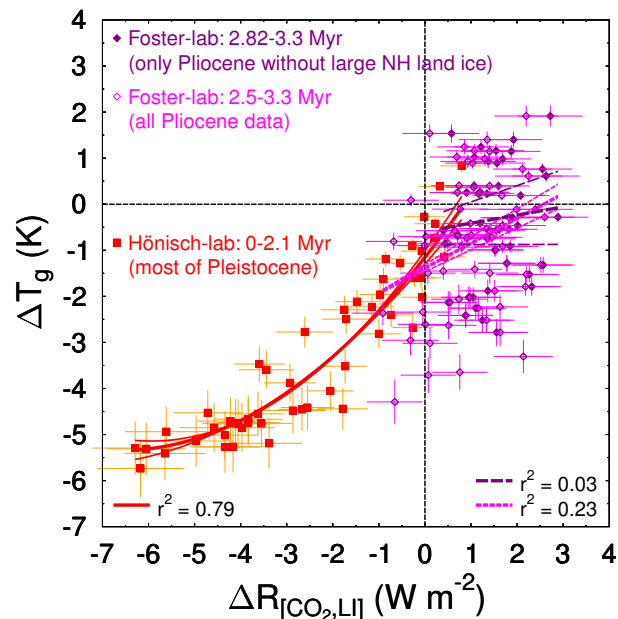


Figure 10. Best-guess 3.3Myr scatter-plot of global temperature change ΔT_g against the radiative forcing of CO_2 and land-ice albedo ($\Delta R_{[\text{CO}_2, \text{LI}]}$). The Hönlisch-lab (Hönlisch et al., 2009) data for the last 2.1 Myr (most of the Pleistocene) and the Pliocene part of the Foster-lab data (Martínez-Botí et al., 2015), complete (2.5–3.3 MyrBP) and only for the almost land-ice free Northern Hemisphere times (2.82–3.3 MyrBP) are compiled to illustrate how the functional dependency between ΔT_g and $\Delta R_{[\text{CO}_2, \text{LI}]}$ changed as function of background climate state.

Title Page

Abstract

Introduction

Conclusions

References

Tables

Figures



Back

Close

Full Screen / Esc

Printer-friendly Version

Interactive Discussion

